Steven A. Brown Special Issue in *European Journal of Neuroscience*:
Dynamic interactions of biological clocks, sleep and metabolism

Title: Circadian clock period length is not consistently linked to chronotype in a wild songbird

Running title: Relationship *tau* and chronotype

Word count: Total count including references and title page: 10,714 words; excluding references: 7,987 words.

Authors: Barbara M. Tomotani*[1,2], Aurelia F. T. Strauß*[1,3], Dmitry Kishkinev[4], Huib van de Haar[1] and Barbara Helm[5**]

** These authors contributed equally to this work.*

*** Submitting author*

[1] Department of Animal Ecology, Netherlands Institute of Ecology (NIOO-KNAW), P.O. Box 50, 6700 AB Wageningen, The Netherlands

[2] Arctic Seasonal Timekeeping Initiative (ASTI), Department of Arctic and Marine Biology, UiT The Arctic University of Norway, PO Box 6050 Langnes, N-9037 Tromsø, Norway

[3] Groningen Institute for Evolutionary Life Sciences (GELIFES), University of Groningen, Nijenborgh 7, 9747 AG Groningen, The Netherlands

[4] School of Life Sciences, Keele University, Newcastle-under-Lyme, Staffordshire, ST5 5BG, United Kingdom

[5] Swiss Ornithological Institute, Seerose 1, 6204 Sempach, Switzerland

ORCID:

BMT: 0000-0002-8855-4803

AS: 0000-0002-6464-9306

DK: 0000-0002-2619-1197

BH: 0000-0002-6648-1463

Acknowledgements

First and foremostly, we thank Steven A. Brown for his enthusiasm, inspiration and support. We greatly regret that our collaboration on “early birds” did not come to full fruition, but aspects of it will carry over to the future. Then, we thank Nadieh Reinders, Lies Bosma and Nivard Boersma for their assistance with fieldwork. We also thank René Janssen for the assistance with setting up the Linnaeusborg receiver and support with equipment, and Kristin Jonasson for assistance with SensorGnome software settings. Ruben de Wit, Anne Dijkzeul, and Nina Teeuw took good care of our birds and also helped with fieldwork. We thank Marcel Visser for support throughout this study and discussions at early stages of the project. BMT was supported by a NWO VENI grant (VI.Veni.192.022) and by the The Arctic Seasonal Timekeeping Initiative (ASTI) grant from UiT strategic funds. AFTS was supported by the Adaptive Life programme of the University of Groningen, the Netherlands.

Abstract (max 250 words)

Circadian clock properties vary between individuals and relate to variation in entrained timing in captivity. How this variation translates into behavioural differences in natural settings, however, is poorly understood. Here we tested in great tits whether variation in the free-running period length (*tau*) under constant dim light (LL) was linked to the phase angle of the entrained rhythm (“chronotype”) in captivity and in the wild, as recently indicated in our study species. We also assessed links between *tau* and the timing of first activity onset and offset under LL relative to the last experienced light-dark (LD) cycle. We kept 66 great tits, caught in two winters, in LL for 14 days and subsequently released them with a radio transmitter back to the wild, where their activity and body temperature rhythms were

tracked for 1 to 22 days. For a subset of birds, chronotype was also recorded in the lab before release. Neither wild nor lab chronotypes were related to *tau*. We also found no correlation between lab and wild chronotypes. However, the first onset in LL had a positive relationship with *tau*, but only in males. Our results demonstrate that links between *tau* and phase of entrainment, postulated on theoretical grounds, may not consistently hold under natural conditions, possibly due to strong masking. This calls for more holistic research on how the many components of the circadian system interact with the environment to shape timing in the wild.

Keywords

Activity rhythm, diel rhythm, telemetry, *tau*, *Parus major*, great tit

1 Introduction

Circadian rhythms are present across the whole tree of life and are considered essential for organisms (Jabbur et al., 2024; Krittika & Yadav, 2020; Woelfle & Johnson, 2009). The rationale for the importance of biological clocks, rather than timing in direct response to the environment, assumes two main advantages. Firstly, circadian rhythms allow for temporal coordination of many, sometimes conflicting, behavioural and physiological processes within an organism. Secondly, circadian rhythms provide an internal reference time by which environmental conditions can be correctly interpreted. Thus, organisms respond appropriately to, and anticipate, naturally cyclic environmental conditions, in particular the variation in natural light and darkness. By entraining their circadian clocks to this major synchronizing cue (*i.e., Zeitgeber*), organisms can tell the time of day and thus anticipate cyclically repeating environmental events (Daan & Aschoff, 1982; Jabbur et al., 2024; Krittika & Yadav, 2020; Pittendrigh, 1958; Woelfle & Johnson, 2009).

Biological clocks exhibit properties of physical oscillators, and these similarities in turn enabled predicting and subsequently experimentally testing clock features (Aschoff & Wever, 1962; Johnson et al., 2003; Pittendrigh & Daan, 1976b; Schmal et al., 2020). When a biological oscillator is synchronized by an entraining cycle, it is expected that the oscillator's intrinsic period length (*i.e., tau*) determines its temporal relationship to the entraining cycle. This relationship is quantified as the timing difference between stable cycle-to-cycle reference points in the rhythms of the oscillator and the entraining cycle, called phases (*e.g.,* start of activity and start of the light phase, respectively). Thus, if the oscillator has a shorter period length than the entraining cycle, the phase angle (*i.e.,* phase of the rhythm minus phase of the entraining cycle) becomes negative, indicating a phase lead of the oscillator (*e.g.,* start of the activity occurs before the start of the light phase), and *vice versa* (Aschoff & Wever, 1962). When this is applied to organisms' activity patterns, typically an individual's activity phase would be predicted by its *tau* relative to the length of the *Zeitgeber* cycle, *e.g.,* a 24-hour light-dark (LD) cycle. Such predictions could indeed be confirmed empirically in the laboratory, for example by manipulation of LD cycles or by using variation in *tau* (Aschoff & Wever, 1962). Still, even under controlled conditions biological oscillators differed from physical oscillators by changing their properties, for example dependent on season or the social setting (Aschoff, 1979).

Importantly, when applied to the natural environment, the predicted relationships between the natural light cycle and an individual's *tau* should contribute to its particular time-keeping in the wild. Properties of circadian clocks, such as *tau*, and consequently phase angle, are variable between species (Daan & Pittendrigh, 1976), between populations of the same species (Daan & Pittendrigh, 1976; Kyriacou et al., 2008) and even between individuals within the same population (Pivarciova et al., 2016; Salmela & Weinig, 2019). In natural populations clock properties should be distributed around the population-specific mean, like most other traits (Daan & Beersma, 2002; Helm & Visser, 2010; Jabbur et al., 2024; Michael et al., 2003; Pittendrigh & Daan, 1976a). In several species, consistent individual patterns of temporal behaviour, such early- versus late-phased activity (i.e., behavioural "chronotypes"), have indeed been described (Roenneberg et al., 2003). In humans these are traditionally assessed via questionnaires (Roenneberg et al., 2003) while in other animals consistent early and late behaviours (*e.g.,* Fleury et al., 2000; Helm & Visser, 2010; Nikhil et al., 2016; Strauß et al., 2022) are used as proxy for distinct chronotypes. Studies of chronotypes have provided mixed evidence for a correlation with *tau*. Where correlations existed, they often explained only small parts of inter-individual differences in chronotype (Dominoni et al., 2013).

The discrepancy between predictions and results, especially in the field, is perhaps not so surprising. In contrast to the laboratory, organisms under natural conditions experience a wide range of environmental inputs that contribute to entrain or modify (*i.e.,* mask) their diel time-keeping (Helm et al., 2017). Main forms of masking are positive masking, which may augment the amplitude of a rhythm, and negative masking, which may suppress it (Mrosovsky, 1999; Schwartz et al., 2017). For example, a nocturnal animal may be kept from displaying nocturnal activity while being exposed to light, and conversely, a diurnal animal may be induced by light to show activity during its circadian rest phase. While masking differs from entrainment by its ephemeral effects during exposure to an external factor, its importance to fitness under natural conditions may equal that of entrainment (Helm et al., 2017; Mrosovsky, 1999; Rotics et al., 2011). Many modifications of time-keeping by either entrainment or masking are mediated by sensory and physiological pathways that jointly control an individual's phase, for example sensitivity to light and ambient temperature, or metabolic or immune state. If there are advantages to organisms in being earlier or later, natural

selection on daily timing should take place and act on any aspects of this integrated circadian system (Helm et al., 2017; Jabbur et al., 2024; Krittika & Yadav, 2020; Roenneberg et al., 2003). Modifications of time-keeping can occur at various levels of the integrated circadian system. For example, when overt behavioural rhythmicity may be absent, rhythmicity could persist in other body function, such as body temperature or gene expression or protein levels incontrol regions of the brain (Beer & Bloch, 2020). Hence, chronobiologists also assess clock properties through other, putatively more robust measures, such as clock gene expression cycles in cell culture (Brown et al., 2005, 2008), or cycles in body temperature (Duffy et al., 2001; Strauß et al., 2022), and apply more indirect approaches such as (clock) gene-phenotype associations (Allebrandt & Roenneberg, 2008).

Arguably the most conclusive test of how the variation in *tau* translates into behavioural differences between animals is to combine measures of clock properties in captivity with measures of chronotype in free-living animals. The number of studies that attempted to do this is limited due to the logistical difficulties of measuring the same individual in the wild and under constant conditions. The studies that succeeded in this attempt also presented mixed results: *i.e.,* in a comparison of urban and rural blackbirds (*Turdus merula*), a positive relationship between *tau* and activity timing was found only in city birds (Dominoni et al., 2013); in female great tits (*Parus major*) a positive relationship was found between incubation activity and *tau* in both city and forest birds (Tomotani et al., 2023), but a previous study with the same species in captivity did not find a relationship (Helm & Visser, 2010; Lehmann et al. 2012).

Therefore, in the present study we aimed for greater clarity by follow-up investigations of the relationship between clock and chronotype, using locomotor activity rhythms and a larger sample of wild, free-living animals. We used the diurnal songbird great tit as a model because its circadian rhythmicity has been extensively studied in captive and wild contexts (de Jong et al., 2016; Helm & Visser, 2010; Lehmann et al., 2012; Spoelstra et al., 2018; Tomotani et al., 2023). We derived *tau* from free-running activity after the rhythms stabilized (from day 2 or later). We then tested whether variation in *tau* was linked to the phase angle of the entrained activity rhythm ("chronotype") in the wild, and for a subset of birds, also in captivity (*i.e.,* "wild chronotype" and "lab chronotype", respectively). In the wild birds, we also quantified diel timing patterns of peripheral body temperature in parallel to their activity patterns from continuous skin temperature measurements using telemetry. Based on oscillator theory summarised above, we expected a positive correlation between *tau* and chronotype.

In addition, we investigated the first activity cycles in constant dim light (LL) separately from subsequent cycles because the phase and period length of the first cycles of the rhythm are affected by *tau* and by the previous conditions that the organism was exposed to (after-effects, Pittendrigh, 1960). We calculated the phase angle of the onset and offset relative to the natural LD cycle experienced by the birds on the previous day. This measure, referred to as first onset and offset in LL, is thought to capture an animal's prediction of morning and evening, based on its previous entrainment, but in the absence of overriding environmental cues, as well as based on effects of *tau* (*e.g.,* Tomotani et al., 2012, 2023). It can thereby tentatively be interpreted as a proxy for the phase angle of an individual's rhythm given its circadian period length, without confounding effects of masking. The measure was previously reported to correlate with *tau* in studies with great tits in captivity (Laine et al., 2019; Spoelstra et al., 2018).

2 Material and Methods

2.1 Measurements in the lab

All experimental procedures in the lab and the field were carried out under licenses of the Animal Experimental Committee of the Royal Netherlands Academy of Sciences (KNAW, protocol NIOO 20.02 128 AVD 80100 2019 9005 / IvD 1356a and NIOO 21.13 / IvD 1963a).

During the winters of 2021 and 2022 we captured wild great tits (Table S1_1) at night, when the birds were roosting in nest boxes. We captured 66 birds in total (including 2 birds captured twice), at the Zernike campus of Groningen (2021, 2022, 53°14.5'N 6°32.3'E), in the city of Utrecht (2021, 52°6.1'N 5°8.9'E) and in Heikamp forest (2021, 52°1.9'N 5°50.3'E). Birds were immediately taken to the Netherlands Institute of Ecology (NIOO-KNAW, 51°59.2'N 5°40.3'E). Once at the institute, birds were ringed, weighed, and in 2021 kept for one day in a cage exactly like the one in the experimental set-up but exposed to the natural LD cycle to acclimatize (Fig. 1). Birds were kept in a room with direct access to natural light, supplemented by indoor lighting (experiencing light intensity values ranging from 120 to 600 lux) that were switched on at sunrise and switched off at sunset. At night birds were kept without any provided light. Birds were then moved from this acclimatization cage to the experimental set-up (Fig. S1_1) the following night. Thus, at the end of the light phase of the preceding LD-cycle, instead of experiencing darkness, birds were exposed to constant dim light (*i.e.,* LL; 0.5 lux at perch level; see Supporting Information Part S1 and Fig. S1_2). Birds were kept in the set-up in LL for 14 days (Fig. 1). In 2022 the capture procedure was the same but birds were placed directly in the set-up. As in 2021, birds were exposed to one natural LD cycle to acclimatize through windows in the room. The set-up was left uncovered until the start of the LL stage. Then, before the following sunset, windows were covered, cage doors were closed at sunset time and the constant dim light treatment started.

The experimental set-up (Fig. S1_1) was designed to measure great tit rhythms. It consisted of individual metal cages, placed in stand-alone plywood racks in groups of six cages (three rows and two columns; Fig. S1_1). The racks provided plywood separators to the outside, as well as between each cage, so that only the metal-barred cage fronts

remained accessible. We then added a wooden front-door that covered the cage fronts except during feeding, effectively isolating the animals from external cues and from each other. A ventilation grid with a light trap on the side of this wooden door provided ventilation. Each cage was individually equipped with a night lamp that provided the dim light continuously for the LL experiment. Cages were also equipped with passive infrared sensors (PIR) that checked for movement every 10 seconds and binned the data every 60 seconds. Thus, the intensity of activity varied from 0 to 6 every 1-min bin (software developed by T&M Automation, Leidschendam, The Netherlands). Throughout the study, the whole room with the isolation cages was kept completely dark, with all windows covered by a thick black plastic. White noise, broadly resembling rain, was played continuously in the background to cover any external noise and animals' vocalizations. Birds were offered *ad libitum* water and food (*i.e.,* beef heart mixture, apple, dry bird food, peanuts, sunflower seeds and live mealworms). Food was refreshed daily but at variable times of the day so that the birds would be unable to use the feeding times as a cue to synchronize their clock. At the end of the experiment, in 2021 birds were returned to a regular cage without recording facilities and were again exposed to the natural LD cycle before being released with a transmitter. In contrast, in 2022 birds were also re-exposed to LD cycles but remained in the set-up prior to release, allowing their re-entrainment to be measured.

2.2 Measurements in the field

To measure biological rhythms in the field, we deployed temperature-sensitive radio transmitters (PicoPip Tag PIP31 & PIP51 Ag317 single celled tag including temperature sensor option, Lotek, Wareham, UK; < 5% of the body weight). Skin temperature measurements have been shown to correlate with core body temperatures in great tits (Nord et al., 2016) to be rhythmic and to deviate from ambient temperatures patterns in winter (Strauß et al., 2022). These transmitters emit pulses of a radio wave, each with a tag-specific frequency (150 – 151 MHz). The detected signal varies in strength with movement and distance of a transmitter so that the variance of signal strength can be used to distinguish active and inactive times of a tagged individual (Dominoni et al., 2014). Additionally, our transmitters were temperature sensitive. The interval between two consecutive pulses depended on the transmitter's temperature so that increasing temperature decreased the pulse interval. This enabled us to simultaneously measure diel skin temperature and activity rhythms (Strauß et al., 2022).

The tags were calibrated before deployment by exposing them to the progressively cooling temperatures of a hot water bath (decreasing from ca. 40°C to 20°C). Temperatures of the water bath were recorded simultaneously with a temperature logger (iButton: Thermochron DS1922L-F5, Maxim, USA), and signals were recorded with a telemetry receiver (SRX800 MD2, Lotek, Wareham, UK).

To record the birds' rhythms, we attached the transmitters to the birds` upper backs (Strauß et al., 2022). If the transmitter is firmly attached to the skin, reliable temperature measurements can be taken. Thus, prior to deployment, we sewed the tags to a cotton cloth (1 cm diameter) to increase gluing and attachment surface. A small patch of feathers on the bird's back was trimmed and the transmitter glued to the patch using eyelash glue and only a small amount of superglue to ensure easy falling-off during moult at the latest. During deployment, the anterior feathers were brushed away and afterwards brushed back in position to cover the patch.

Individuals were automatically recorded using stationary receivers. The receivers were self-constructed using materials of Motus (a collaborative wildlife radio tracking system, Taylor et al., 2017) and the SensorGnome (SG) system (here, Raspberry Pi3 model B, Raspberry Pi Foundation, Cambridge, UK) with software version 2018-10-12 (SensorGnome Project, 2018). One to two SGs were placed per site, each with an omnidirectional antenna (SIRIO CX 148 U – 148-152 MHz, Volta Mantovana, Italy). In Groningen we additionally used a fixed station on the roof of the university building "Linnaeusborg" (RUG) that had five directional antennas (SIRIO WY 140-6N, SIRIO Antenne, Volta Mantovana, Italy). The receivers were set to scan through the frequencies of each deployed tag for 10 sec before switching to the next frequency, so every tag was recorded in intervals of 1.5 – 2.8 min (see Supporting Information Part S2 for more details).

2.3 Data processing

The captivity data were used to obtain a) the first onset and offset in LL (2021 and 2022), b) the bird`s endogenous free-running period length *tau*, and c) onsets and offsets of the re-entrained rhythm (lab chronotype, 2022 only) (Fig. 1). All 66 individual actograms are shown in Figures S3 – S10.

To account for seasonal changes in day length, we calculated relative timing by subtracting the time of sunrise or sunset from the activity onset and offset time, respectively (*i.e.,* activity onset minus sunrise or activity offset minus sunset). Thus, a bird would have a negative onset phase angle if its activity started before sunrise and a positive onset phase angle if its activity started after sunrise. Likewise, it would have a negative offset phase angle if its activity ended before sunset and a positive offset phase angle if its activity ended after sunset.

The data collected from the set-up were used to produce actograms using the software *Chronoshop* (v. 1.04, 2015, written by Spoelstra, *e.g.,* Spoelstra et al., 2018; Tomotani et al., 2023). *Chronoshop* was also used for obtaining the values of *tau*, and onset and offset of activity. *Tau* was calculated via the Sokolove & Bushell method (S-B), for all but

one bird in which no clear periodicity emerged. In these analyses, we excluded the first cycle that we used to obtain the first onset and offset in LL. We also excluded additional cycles when the rhythm was still displaying after-effects (see Supporting Information). In these excluded cycles the rhythm was still similar to the previous synchronized state with a period close to 24 hours, and the onset of activity was matching the time of sunrise. This lasted from 1 to 7 days depending on the individual, and was easily detected by a change in the actogram where the onset of activity drifted from the synchronized onset (see Fig. 1). For example, in Figure 1 (with annotations on the right), cycle 0 is the synchronized onset under a LD cycle, cycles 1 to 3, when the animal had transitioned to LL, show history-dependent after-effects from the previous synchronization, whereby onset time is similar to the entrained state. The onsets start to drift from cycle 4 onwards as the animal expresses its own internal period length. For extracting the onset and offset of activity, the software calculates the centre of gravity per cycle positioned at the mean vector angle. Then, it estimates the activity onset or offset by going 0.5 cycles back or forward in time, respectively, to detect the phase when the momentary activity first exceeds the average activity in the current cycle. In order to avoid onsets and offsets being detected at timewhere small amounts of movements or noise are present, a running mean is fit to the data so only activity bins above those values are classified as the onset or offset of activity (Spoelstra et al., 2018). Because the detection of the onset and offset was sensitive to the activity level of the individual bird, we had to adjust the running mean per individual, per cycle, varying between 10 bins (48 onsets / 32 offsets), 70 bins (14 onsets / 26 offsets) or 180 bins (0 onsets / 4 offsets). In a few instances, the amount of background noise did not allow the detection of an onset or offset of activity regardless of the running mean used, in such instances the onset for that cycle was excluded. The estimation of *tau* is very robust to small amounts of noise in the activity rhythms and was not affected by changing the running mean.

From the wild, we obtained telemetric data that were processed and filtered in R (version 4.3.1, R Core Team, 2023) and R studio (version 2023.06.2) to obtain activity and skin temperature estimates (for details see Supporting Information Part S2 Section 1 – 4). The raw data were filtered to address several issues associated with the data collection using a SG. In particular, we accounted for carry-over effects from switching from one to the next frequency, due to a time lag between transitioning in the hard- and software. We also accounted for multiple detections per second due to multiple recordings of the same radio frequency along the antenna and for further artefacts visible in the recorded frequency and background noise that were probably caused by the SG software (for details, see Supporting Information Part S2 Section 3). Thereafter, we calculated pulse intervals and applied the tag-specific calibration curves to calculate the skin temperature sensed by the transmitter (Jonasson, 2017). We binned the data into 5-min bins and calculated the deviation of signal strength between two consecutive bins as an indicator of activity.

To extract the onset and offset of activity we used a behavioural changepoint analysis (BCPA) that finds the most plausible changepoint by fitting two distributions to the data (Dominoni et al., 2014; Strauß et al., 2022, for details see Supporting Information Part S2, Section 5, Fig. S2_5). We selected an 8-hour window around 7:20 CET (*i.e.,* the overall mean onset of activity across the whole dataset) for onsets and around 18:20 CET (*i.e.,* the overall mean offset of activity) for offsets. For the BCPA, we set a 70%-threshold to make sure that enough data were available for a reliable analysis. In 158 occasions (67 onsets and 91 offsets), a BCPA was not possible. The birds were recorded well at the night-time but had many data gaps during their active phase. Therefore, we additionally used the first and last intersection of a 4dB-threshold on a given day (Adelman et al., 2010) to determine activity onset and offset, respectively, when enough data were available at night-time (*i.e.,* > 70% between midnight and sunrise or sunset, respectively). Chronotypes from the BCPA and from the 4dB-threshold were highly correlated in the cases were both methods could be used (onset: Pearson's cor = 0.94, confidence interval = (0.93, 0.96), t = 40.21, df = 197, $p << 0.001$; offset: Pearson's cor = 0.87, confidence interval = (0.82, 0.90), t = 19.69, df = 127, $p << 0.001$). To assess the skin temperature minimum at night, we smoothed the temperature data, averaged to 5-min bins, using a 3-harmonic sinusoidal curve (Strauß et al. 2022, for details see Supporting Information Part S2 Fig. S2_4.2 in Section 4), and interpolated for data gaps of maximally three bins (*i.e.,* 15 min). We selected a 12-hour window around the observed overall mean time of minimum temperature at 4:10 CET, derived from the data from all birds. From the smoothed data, we then extracted for each bird the time of the minimum temperature just before rewarming for its active phase (adjusted from Strauß et al. 2022, for details see Supporting Information Part S2, Section 5). The time of temperature minimum was interpreted as the onset of the anticipatory increase in body temperature prior to wakening.

2.4 Data analysis

The birds used in this study differed in their origins (caught in distinct sites and years) and we also had males and females. In order to test if this would have an impact on our measures, we first explored the variation of *tau*, using one *tau* measurement per individual (n = 63, using only one *tau* estimate per bird), in response to the covariates *group* and *sex*. We also accounted for cage position in the experimental set-up by including rack as random factor to account for the possibility that the six cages in the same rack could be more similar to one another than to the other cages in the room. As there were significant differences between *groups and sexes, we included group and sex in all following models (Fig. S1_11 & Table S1_2). In all cases, we combined year and site to create four groups (i.e., Groningen 2021: 6 females, 8 males; Utrecht 2021: 4 females, 10 males; Heikamp 2021: 7 females, 8 males; Groningen 2022: 10 females, 14 males, Table S1_1) due to the unbalanced study design.*

We then assessed the relationship between *tau*, chronotype measured in the wild and in the lab, and first onset or offset in LL. Models included as response variables chronotypes (*i.e.,* measures of the entrained clock using onset and offset in minutes relative to sunrise or sunset) measured either in the lab (Fig. 1b) or in the wild (Fig. 1c), or the first activity onset or offset in LL (Fig. 1a). *Tau* was used as an explanatory variable in all models, while models with chronotypes as response variables also included the first onset or offset in LL as an explanatory variable. Analyses were done in separate linear mixed models with Gaussian error distribution (*lme4* package, Bates et al., 2015). Models included *Individual* as random factor to account for multiple measurements and for studying between-individual differences in chronotype. To assess individual variation, the proportional variance (σ^2) of the *Individual* term was calculated from the model output. All test statistics were obtained via stepwise model reduction using likelihood ratio tests (*drop1* and *anova* function). Estimates were extracted from the model with all non-significant interactions dropped.

For the wild chronotype traits (*i.e.,* activity onset and offset, and time of skin temperature minimum collected in the wild), we excluded the first day after release into the wild to avoid confounding effects from the disrupted night of release. We then chose data from Groningen only (both years), because too few individuals were recorded at the other sites (four in Utrecht, one in Heikamp). As before, we assessed sex- and group-specific relationships with *tau* and onset and offset in LL, and also included Julian day and mean ambient temperature (at night for onset and at daytime for offset) to account for seasonal and temperature-dependent variation (temperature data from the weather station in Elde, (Royal Netherlands Meteorological Institute (KNMI), 2023)). To assess a potential correlation between the times of activity onset and skin temperature minimum, we extracted individual-specific residual variances (best linear unbiased predictor, BLUP) to account for multiple measurements. In order to obtain the BLUPs, we used the same model as from above for both traits, including only days when timing of both, activity and skin temperature minimum, were available (n=167). We then used the BLUPs to check for a correlation between chronotype estimated from activity and skin temperature (Houslay & Wilson, 2017). Because the analysis of BLUP correlation is prone to false positives, multivariate models are preferable, but sample sizes in our study were insufficient for multivariate analyses (Houslay & Wilson, 2017). Thus using BLUPs, we found no significant relationship and expect therefore that the analysis, here, was not delivering false positives.

For tests involving the first onset or offset in LL or lab chronotypes as responses to *tau*, we included *group*, *sex* and their two-way interactions with *tau* as covariates. Lab chronotype was only available for Groningen 2022 and its analysis also included the interaction between first onset and offset in LL and *sex*. Then, in separate *post hoc* models, we verified effects of *tau* for males and females.

Finally, as a separate test, we compared if wild chronotype traits were related to lab chronotype using the subset of individuals from 2022 for which both measures were available. In two separate models we modelled the onset and offset of activity in the wild as response variables. We included as predictors the mean onset or offset in captivity, *sex* and their interaction, as well as Julian day and mean ambient temperature of night or day, and *individual* as random effect.

3 Results

The free-running period lengths *tau* for the 63 individuals in our studies ranged from 23 to 24.7 h, and were on average shorter than 24 h (mean 23.75 ± 0.04 h; Fig. S1_11 & Table S1_2). Day-to-day changes in the timing of onset under LL are shown in Figure S1_12. We found that the wild chronotype measures, both in terms of activity onset and offset, were unrelated to *tau* (slope for onset: -11 min per h, $F_{1,222} = 1.45$, p = 0.25; offset: 0 min per h, $F_{1,177} = 0.00$, p = 0.98, Fig. S1_2 & Table S1_3). However, individuals differed significantly from each other in wild chronotype (onset: 0.34 proportional variance (σ^2), $X^2_{1,n=223} = 23.30$, p << 0.001; offset: $\sigma^2 = 0.32$, $X^2_{1,n=178} = 14.74$, p < 0.001). For the birds of 2022, whose chronotype was also measured in the lab, we found that both activity onset and offset were unrelated to *tau* (slope for onset: -2 min per h, $F_{1,118} = 0.07$, p = 0.80; offset: 5 min per h, $F_{1,110} = 3.01$, p = 0.10, Fig. 2 & Table S1_4), but that these individuals also differed consistently from each other (onset: $\sigma^2 = 0.33$, $X^2_{1,n=119} = 8.52$, p = 0.004; offset: $\sigma^2 = 0.40$, $X^2_{1,n=111} = 19.92$, p << 0.001, Table S1_4). In these birds, chronotype measured in the wild could not be explained by chronotype measured in the lab (onset: -1 min per min, $F_{1,142} = 0.30$, p = 0. 60; offset: 0 min per min, $F_{1,124} = 0.13$, p = 0.73, Table S1_5).

The relationship between the first onset in LL and *tau* depended on *sex* ($F_{1,59} = 4.23$, p = 0.04, Fig. 3 and Table S1_6). Specifically, in males, the first onset in LL was significantly positively related to *tau*, so that males delayed onset by 45 min per hour of longer *tau* (*post hoc*: $F_{1,34} = 5.58$, p = 0.02). No significant relationship was detected in females (*post hoc*: -10 min per h, $F_{1,24} = 0.27$, p = 0.61, Table S1_7). First offset in LL was also positively, but not significantly, related to *tau* such that offset was delayed with increasing *tau* (slope of 78 min per h, $F_{1,60} = 2.79$, p = 0.10). For the offset, we found no effects of *sex* ($F_{1,60} = 2.96$, p = 0.09) and of its interaction with $tau_{1,60} = 0.03$, p = 0.85, Table S1_6). First onset or offset in LL were not significantly related to entrained onset and offset of activity, neither in the wild (onset: 0 min per min, $F_{1,222} = 3.08$, p = 0. 10; offset: 0 min per min, $F_{1,177} = 0.20$, p = 0.66) nor in the lab (onset: 2 min per min, $F_{1,118} = 0.15$, p = 0.71; offset: -1 min per min, $F_{1,110} = 1.50$, p = 0.24).

For time of the skin temperature minimum, we also failed to detect significant relationships with predictors. There was no relation with *tau* (slope: -23 min per h, $F_{1,158}$ = 2.13, p = 0.20, Fig. S1_13 & Table S1_8) and with first onset in LL (slope: 1 min per min, $F_{1,158}$ = 4.83, p = 0.10), nor with lab chronotype in the subset of the 2022 birds (slope: -3 min per min, $F_{1,119}$ = 0.97, p = 0.37). Timing of the skin temperature minimum also did not differ between individuals (σ^2 = 0.02, $X^2_{1,n=159}$ = 0.00, p = 1.00, Table S1_8). Further, we could not find a correlation between the timings of activity in the wild and of skin temperature minima (correlation of BLUPs: Pearson's cor = -0.06, confidence interval = (-0.50, 0.41), t = -0.24, df = 17, p-value = 0.82, Fig. S1_13).

4 Discussion

In our study, we confirmed that while free-living great tits displayed individual chronotypes under entrained conditions, these chronotypes were unrelated to *tau*. The lack of a relationship contrasts with what has been postulated in earlier theoretical and laboratory studies and thus adds to the evidence that predictions made using lab animals may not consistently hold in the wild (Calisi & Bentley, 2009; Daan, 2011; Daan et al., 2011; Tomotani et al., 2012). Earlier studies of the same species also yielded inconsistent results. A large-scale captivity study of hand-raised great tits and follow-up research involving temperature manipulations also reported that *tau* was unrelated to chronotype in the lab in the birds' first autumn of life (Helm & Visser, 2010; Lehmann et al., 2012). Conversely, a recent, smaller-scale study of incubation rhythms revealed that activity onset of wild female great tits did correlate with *tau* (Tomotani et al. 2023). Such inconsistent findings are perhaps not surprising given the complex interactions between the circadian system and the environment (Helm et al., 2017).

Classical laboratory studies showed systematic relationships between *tau* and phase of entrainment, leading to the formulation of "rules" on theoretical grounds (Floessner & Hut, 2017). Such conclusions were particularly based on testing ranges of entrainment and manipulating the period length of the *Zeitgeber* (Aschoff, 1980). Chronobiologists studying humans also attempted to link chronotype with *tau* (*e.g.,* Allebrandt & Roenneberg, 2008; Brown et al., 2008; Duffy et al., 2001), and in some cases, showed the expected positive correlations between longer *tau* and later chronotype. Intriguingly, Steve Brown and co-authors showed that *tau* also correlated with a molecular measure for chronotype, the entrained phase of a reporter on a clock gene in cultured dermal fibroblasts (Brown et al., 2008). Positive correlations between longer *tau* and later chronotype have also sometimes been found in wild and wild-derived animals (Fleury et al., 2000; Nikhil et al., 2016; Wicht et al., 2014). However, the evidence has been mixed for birds, including as mentioned above for great tits. While Tomotani et al. (2023), and also Dominoni et al. (2013), showed a relationship between *tau* and chronotype or activity phase in at least some populations, other studies failed to do so (Helm & Visser 2010, Lehmann et al. 2012). One possible explanation for such discrepancy relateso *tau* as estimated during LL. Despite the fact that the variation in *tau* has a genetic basis (Konopka & Benzer, 1971) and a high heritability (Helm & Visser, 2010), period length is still a labile trait (Pittendrigh & Daan, 1976a). *Tau* has been reported to change seasonally (Aschoff, 1979; Pohl, 1972; Gwinner, 1975; but see Dixit & Singh, 2016) and is affected by changes in light intensity (*e.g.,* Pohl, 1974) and previous entrainment (*i.e.,* after-effects Pittendrigh, 1960), as well as by other aspects such as housing conditions and hormones (Aschoff, 1979).

Despite lacking correlations between *tau* and chronotype, our study provides some support for links between *tau* and phase of entrainment. We found that in males, but not in females, the first onset of activity in LL correlated positively with *tau*. The first onset in LL can be interpreted as approximating the phase angle of entrainment of an individual with a given free-running period length in the absence of masking. This is because on one hand, the first day(s) after moving an animal from entrained to constant conditions often show after-effects of the previous entrainment on period, phase, and amplitude (Fig. S1_12) that are missing in later stages of a stabilized free-running rhythm (Pittendrigh, 1960). On the other hand, these after-effects take place during exposure to constant conditions, when all external influences on timing are removed and activity can occur at the entrained phase it would assume without masking. That correlations with *tau* are nonetheless weak is perhaps expected since history-dependent after-effects are a combined reflection of *tau*, of previous entrainment and of other influences on the response of organisms to altered light conditions (Pittendrigh & Daan, 1976a). We thus found a discrepancy between lacking correlations of *tau* with chronotype and some correlation of *tau* with first activity timing in LL. This discrepancy might indicate strong effects of masking in the wild. Chronotype under natural, masking conditions would therefore arise from influences on timing other than of circadian period length.

The conclusions from males are weakened by the lack of an association of *tau* and first onset in LL in females, as well as by non-significant associations of *tau* with first offset in LL. However, sex differences in activity patterns and circadian rhythms have been previously reported (Helm & Visser, 2010; Stuber et al., 2015; Walton et al., 2022). Thus, sex-specific differences in the clock-chronotype link could stem from selection pressures that differentially affect phase and masking responses, as shown for example in fruit flies (Ghosh et al., 2021). Furthermore, although not significant, in both sexes *tau* was positively associated with first offset of activity in LL. The weakness of this association could be due to the large variation in offset derived from our birds. As evident from individual actograms (Figs. S1_3 – S10), there was a tendency for the evening component of activity to dissociate from the morning component, leading to highly divergent timings of activity offset. Nonetheless, we maintain that after-effects could be interesting for studies with wild animals as they can reveal aspects of entrainment in the wild. Animals under constant conditions in the absence of masking may retain – at least for a few cycles – the same period length and phase of their

entrained state (Fig. S1_12). Therefore, after-effects could arguably serve as a closer measure of the clock-predictive ability of the animal than its entrained activity rhythm (Oda & Valentinuzzi, 2023; Tomotani et al., 2012, 2023).

In addition to masking, environmental factors modify the entrained rhythm also in other ways, for example via modulations of clock amplitude and robustness (Daan & Pittendrigh, 1976; Oda & Valentinuzzi, 2023; Pittendrigh & Daan, 1976c, 1976b; Schmal et al., 2015), via modulations of sensory input and output pathways (Chellappa, 2021; Gwinner et al., 1997; Schmal et al., 2020; Shimmura et al., 2017) or via effects of other oscillators (Bartell & Gwinner, 2005; Gänshirt, et al., 1984; Mistlberger, 1994; van der Vinne et al., 2014). The strength of photic entrainment may change due to either environmental changes in exposure to light or to organismic changes in light sensitivity (Marimuthu, 1984; Schmal et al., 2015, 2020). Although chronotype is broadly consistent within individuals, as also shown in our study (Schwartz et al., 2017), various environmental variables may modify timing. For example, at higher latitudes, winter has a much shorter light phase (*i.e.,* day length) and lower light intensity than summer. Thus, some models have predicted the strength of the entrainment to be weaker in winter, possibly allowing the vriation in chronotypes to be larger (Schmal et al., 2020). Modifying effects can arise from other environmental factors such as light pollution (Sanders et al., 2021), ambient temperature (Lehmann et al., 2012), reproductive stage, season (Daan & Aschoff, 1975; Strauß et al., 2024), social cues (Davidson & Menaker, 2003), and sound (Dominoni et al., 2020). It is noteworthy that the two cited avian studies that showed links between *tau* and chronotype did so for birds experiencing reduced perceived strength of the Zeitgeber. Dominoni et al. (2013) found a relationship only in an urban habitat (Dominoni et al., 2013), where light pollution could result in a reduced contrast between the light and dark phases. This weaker *Zeitgeber* in cities could thus lead to greater variation in chronotypes. Furthermore, Tomotani et al. (2023) had derived chronotype of females during the incubation phase when nest box-breeding females experience greatly reduced exposure to day light. This reduced Zeitgeber amplitude may contribute to greater expression of inter-individual differences. Some of these environmental factors may have contributed to the inconsistent findings in the case of the great tit.

By which traits chronotype and the circadian clock are measured may also impact the results (*e.g.,* Roenneberg et al., 2003). It is possible that results differ when using other physiological processes (*e.g.,* melatonin levels, *e.g.,* Zawilska et al., 2006, body temperature *e.g.,* Strauß et al., 2022, gene expression or protein levels, e.g., Beer & Bloch, 2020) or other behaviours than the locomotor rhythm (incubation behaviour, *e.g.,* Tomotani et al., 2023). While a relationship should be expected between the different rhythms, there is ample room for variation. Physiological rhythms such as melatonin and (core) body temperature are often considered a more precise way of assessing the phase of entrainment (Roenneberg, 2012; Strauß et al., 2022). In our present study, the timing of the increase in peripheral body temperature during early morning was also unrelated to activity-derived *tau*. The low accuracy of determining phase markers of the measured body temperature rhythm (*i.e.,* timing of the temperature minimum) made it less precise than the activity rhythm, thus further blurring the relationship between clock and chronotype. We cannot exclude that in our birds, other measures of both chronotype or *tau*, might have revealed different findings.

How does variation in clock relate to variation in behaviour then? As discussed above, it is perhaps not surprising that theoretical predictions are not consistently met in the natural environment. The clock *versus* behaviour relationship in the wild is more tenuous due to direct influences of the environment on the behaviour itself and to differences between organisms in all of the implicated pathways. *Tau* is only one feature of the circadian rhythms and, although it affects other properties such as the shape of phase response curves (Daan & Pittendrigh, 1976), its influence is subject to many factors that jointly exert phase control. Next to the phase set by the clock relative to the environment, multiple levels of organization ultimately lead to variation of rhythms in nature (Helm et al., 2017).

5 Conclusion

Our study shows that variation in *tau* is not consistently related to chronotype in the great tit. Because the variation in both *tau* and chronotype depends on environmental and internal state conditions, the relationship between clock and chronotype may only appear in certain circumstances, times of the year, or in specific traits. If this is true, literature support of a seemingly straight-forward relationship could also be a result of reporting bias. However, evidence for individual differences in chronotype and in diel behaviour, including those reported here, indicates that the suite of components of the circadian system interact with the environment to form broadly consistent temporal behaviour. For wild animals, such consistency matters, especially because of a possible link between chronotype and fitness (Martorell-Barceló et al., 2018; Womack et al., 2023). From an ecological perspective, the important question now is which are the other factors – beside the clock's free-running period length – that explain variation in chronotype and diel timing of behaviour. To solve this challenge, we reaffirm that studying clock features particularly through the combination of measurements in captivity and in the natural settings will be crucial for going forward. A holistic approach, as always embraced by Steven Brown, will benefit chronobiologcal, ecological and behavioural research alike.

List of Abbreviations

LD: light-dark cycle

LL: constant dim light

Tau: length of the free-running period under constant dim light

Figure Legends

Figure 1: Actogram of one of the birds from the 2022 group, showing the measurements collected in this study. Activity (amount of activity per minute measured in increments of 10 seconds, thus ranging from 0 to 6 per 1-min bin) is plotted in black against time of day, whereby each row represents a day of experiment. Activities on a given day are repeated to the right of each day (i.e., double-plotted) for greater clarity. Measures are as follows: **a)** First onset and offset in LL (constant dim light conditions). **b)** Tau, the period length of the endogenous clock. **c)** Lab chronotype, the onsets and offsets of the rhythm in captivity, once re-synchronized by a light-dark (LD) cycle, based on a subset of birds. **d)** Wild chronotype, the onsets and offsets of the activity rhythm and body temperature in the wild (data not shown).

Figure 2: Relationships between free-running period length *tau* and activity onset (left) and offset (right) in the wild and in captivity. Top: wild chronotype, i.e., onset or offset in the wild relative to sunrise and sunset after release (only Groningen 2021 and 2022). Bottom: lab chronotype, i.e., onset or offset in captivity under light-dark cycles (LD) relative to lights-on and lights-off, respectively (based on data only collected in Groningen 2022). Raw data are shown as means with standard errors for every individual and model estimates are presented as lines with 95% confidence interval. Colours represent different groups, shapes represent sex (circles in females, triangles in males), and line types show significance level: solid for $p < 0.05$, dotted for not significant.

Figure 3: Relationships between free-running period length *tau* and the first activity onset (left) and offset (right) in constant dim light (LL) relative to lights-on and lights-off, respectively, on the preceding day in females (top) and males (bottom). Raw data are shown for every individual and model estimates are presented as lines with 95% confidence interval. Colours represent different groups, shapes represent sex (circles in females, triangles in males), and line types show significance level: solid for $p < 0.05$, dotted for not significant. A significant relationship was only found for first onset in LL in males.

Author contributions

BMT: Conceptualization, Data curation, Funding acquisition, Investigation, Project administration, Supervision, Visualisation, Writing - original draft, Writing - review and editing. AS: Conceptualization, Data curation, Formal analysis, Investigation, Methodology, Visualisation, Writing - original draft, Writing - review and editing. DK: Methodology, Software, Writing - review and editing. HH: Investigation, Writing - review and editing. BH: Conceptualization, Funding acquisition, Methodology, Investigation, Supervision, Writing - original draft, Writing - review and editing.

Conflict of interest statement

The authors declare no conflicts of interest.

Data Availability Statement

Dataset and code used in this manuscript are available as Figshare repository (https://doi.org/10.6084/m9.figshare.26090455).

References

Adelman, J. S., Córdoba-Córdoba, S., Spoelstra, K., Wikelski, M., & Hau, M. (2010). Radiotelemetry reveals variation in fever and sickness behaviours with latitude in a free-living passerine. *Functional Ecology*, *24*(4), 813–823. https://doi.org/10.1111/j.1365-2435.2010.01702.x

Allebrandt, K. V., & Roenneberg, T. (2008). The search for circadian clock components in humans: New perspectives for association studies. *Brazilian Journal of Medical and Biological Research = Revista Brasileira De Pesquisas Medicas E Biologicas*, *41*(8), 716–721. https://doi.org/10.1590/s0100-879x2008000800013

Ardia, D. R., Cooper, C. B., & Dhondt, A. A. (2006). Warm temperatures lead to early onset of incubation, shorter incubation periods and greater hatching asynchrony in tree swallows Tachycineta bicolor at the extremes of their range. *Journal of Avian Biology*, *37*(2), 137–142. https://doi.org/10.1111/j.0908-8857.2006.03747.x

Aschoff, J. (1979). Circadian Rhythms: Influences of Internal and External Factors on the Period Measured in Constant Conditions. *Zeitschrift Für Tierpsychologie*, *49*(3), 225–249. https://doi.org/10.1111/j.1439-0310.1979.tb00290.x

Aschoff, J. (1980). Ranges of entrainment: A comparative analysis of circadian rhythm studies. *Proceedings of the XIIIth Conference of the International Society of Chronobiology*, 105–112.

Aschoff, J. (1988). Masking of circadian rhythms by zeitgebers as opposed to entrainment. *Trends in Chronobiology*, 149–161.

Aschoff, J., & Wever, R. (1962). Über Phasenbeziehungen zwischen biologischer Tagesperiodik und Zeitgeberperiodik. *Zeitschrift Für Vergleichende Physiologie*, *46*(2), 115–128.

Bartell, P. A., & Gwinner, E. (2005). A Separate Circadian Oscillator Controls Nocturnal Migratory Restlessness in the Songbird Sylvia borin. *Journal of Biological Rhythms*, *20*(6), 538–549. https://doi.org/10.1177/0748730405281826

Bates, D., Mächler, M., Bolker, B., & Walker, S. (2015). Fitting Linear Mixed-Effects Models Using lme4. *Journal of Statistical Software*, *67*(1), 1–48.

Beer, K., & Bloch, G. (2020). Circadian plasticity in honey bees. *The Biochemist*, *42*. https://doi.org/10.1042/BIO04202002

Brown, S. A., Fleury-Olela, F., Nagoshi, E., Hauser, C., Juge, C., Meier, C. A., Chicheportiche, R., Dayer, J.-M., Albrecht, U., & Schibler, U. (2005). The Period Length of Fibroblast Circadian Gene Expression Varies Widely among Human Individuals. *PLOS Biology*, *3*(10), e338. https://doi.org/10.1371/journal.pbio.0030338

Brown, S. A., Kunz, D., Dumas, A., Westermark, P. O., Vanselow, K., Tilmann-Wahnschaffe, A., Herzel, H., & Kramer, A. (2008). Molecular insights into human daily behavior. *Proceedings of the National Academy of Sciences*, *105*(5), 1602–1607. https://doi.org/10.1073/pnas.0707772105

Calisi, R. M., & Bentley, G. E. (2009). Lab and field experiments: Are they the same animal? *Hormones and Behavior*, *56*(1), 1–10. https://doi.org/10.1016/j.yhbeh.2009.02.010

Chellappa, S. L. (2021). Individual differences in light sensitivity affect sleep and circadian rhythms. *Sleep*, *44*(2), zsaa214. https://doi.org/10.1093/sleep/zsaa214

Cooper, C. B., Hochachka, W. M., Butcher, G., & Dhondt, A. A. (2005). Seasonal and Latitudinal Trends in Clutch Size: Thermal Constraints during Laying and Incubation. *Ecology*, *86*(8), 2018–2031. https://doi.org/10.1890/03-8028

Daan, S. (2011). How and Why? The lab versus the field. *Sleep and Biological Rhythms*, *9*(1), 1–2. https://doi.org/10.1111/j.1479-8425.2010.00482.x

Daan, S., & Aschoff, J. (1975). Circadian rhythms of locomotor activity in captive birds and mammals: Their variations with season and latitude. *Oecologia*, *18*(4), 269–316. https://doi.org/10.1007/BF00345851

Daan, S., & Aschoff, J. (1982). Circadian Contributions to Survival. In J. Aschoff, S. Daan, & G. A. Groos (Eds.), *Vertebrate Circadian Systems* (pp. 305–321). Springer Berlin Heidelberg.

Daan, S., & Beersma, D. G. M. (2002). Circadian Frequency and Its Variability. In V. Kumar (Ed.), *Biological Rhythms* (pp. 24–37). Springer. https://doi.org/10.1007/978-3-662-06085-8_3

Daan, S., & Pittendrigh, C. S. (1976). A functional analysis of circadian pacemakers in nocturnal rodents II. The Variability of Phase Response Curves. *Journal of Comparative Physiology*, *106*(3), 253–266. https://doi.org/10.1007/BF01417857

Daan, S., Spoelstra, K., Albrecht, U., Schmutz, I., Daan, M., Daan, B., Rienks, F., Poletaeva, I., Dell'Omo, G., Vyssotski, A., & Lipp, H. P. (2011). Lab mice in the field: Unorthodox daily activity and effects of a dysfunctional circadian clock allele. *Journal of Biological Rhythms*, *26*(2), 118–129. https://doi.org/10.1177/0748730410397645

Davidson, A. J., & Menaker, M. (2003). Birds of a feather clock together – sometimes: Social synchronization of circadian rhythms. *Current Opinion in Neurobiology*, *13*(6), 765–769. https://doi.org/10.1016/j.conb.2003.10.011

de Jong, M., Jeninga, L., Ouyang, J. Q., van Oers, K., Spoelstra, K., & Visser, M. E. (2016). Dose-dependent responses of avian daily rhythms to artificial light at night. *Physiology & Behavior*, *155*, 172–179. https://doi.org/10.1016/j.physbeh.2015.12.012

Dixit, A. S., & Singh, N. S. (2016). Seasonality in circadian locomotor activity and serum testosterone level in the subtropical tree sparrow (Passer montanus). *Journal of Photochemistry and Photobiology. B, Biology*, *158*, 61–68. https://doi.org/10.1016/j.jphotobiol.2016.02.014

Dominoni, D. M., Carmona-Wagner, E. O., Hofmann, M., Kranstauber, B., & Partecke, J. (2014). Individual-based measurements of light intensity provide new insights into the effects of artificial light at night on daily rhythms of urban-dwelling songbirds. *Journal of Animal Ecology*, *83*(3), 681–692. https://doi.org/10.1111/1365-2656.12150

Dominoni, D. M., Helm, B., Lehmann, M., Dowse, H. B., & Partecke, J. (2013). Clocks for the city: Circadian differences between forest and city songbirds. *Proceedings of the Royal Society of London B: Biological Sciences*, *280*(1763), 20130593. https://doi.org/10.1098/rspb.2013.0593

Dominoni, D. M., Smit, J. A. H., Visser, M. E., & Halfwerk, W. (2020). Multisensory pollution: Artificial light at night and anthropogenic noise have interactive effects on activity patterns of great tits (Parus major). *Environmental Pollution*, *256*, 113314. https://doi.org/10.1016/j.envpol.2019.113314

Duffy, J. F., Rimmer, D. W., & Czeisler, C. A. (2001). Association of intrinsic circadian period with morningness-eveningness, usual wake time, and circadian phase. *Behavioral Neuroscience*, *115*(4), 895–899. https://doi.org/10.1037/0735-7044.115.4.895

Fleury, F., Allemand, R., Vavre, F., Fouillet, P., & Boulétreau, M. (2000). Adaptive significance of a circadian clock: Temporal segregation of activities reduces intrinsic competitive inferiority in Drosophila parasitoids. *Proceedings of the Royal Society of London. Series B: Biological Sciences*, *267*(1447), 1005–1010. https://doi.org/10.1098/rspb.2000.1103

Floessner, T. S. E., & Hut, R. A. (2017). Basic Principles Underlying Biological Oscillations and Their Entrainment. In *Kumar V (ed) Biological Timekeeping: Clocks, Rhythms and Behaviour.* (pp. 47–58). Springer. https://doi.org/10.1007/978-81-322-3688-7_3

Gänshirt, G., Daan, S., & Gerkema, M. P. (1984). Arrhythmic perch hopping and rhythmic feeding of starlings in constant light: Separate circadian oscillators? *Journal of Comparative Physiology A*, *154*(5), 669–674. https://doi.org/10.1007/BF01350220

Ghosh, A., Sharma, P., Dansana, S., & Sheeba, V. (2021). Evidence for Co-Evolution of Masking With Circadian Phase in Drosophila Melanogaster. *Journal of Biological Rhythms*, *36*(3), 254–270. https://doi.org/10.1177/0748730421997262

Gwinner, E. (1975). Effects of season and external testosterone on the freerunning circadian activity rhythm of european starlings (Sturnus vulgaris). *Journal of Comparative Physiology*, *103*(3), 315–328. https://doi.org/10.1007/BF00612024

Gwinner, E., Hau, M., & Heigl, S. (1997). Melatonin: Generation and Modulation of Avian Circadian Rhythms. *Brain Research Bulletin*, *44*(4), 439–444. https://doi.org/10.1016/S0361-9230(97)00224-4

Haftorn, S. (1988). Incubating Female Passerines Do Not Let the Egg Temperature Fall below the "Physiological Zero Temperature" during Their Absences from the Nest. *Ornis Scandinavica (Scandinavian Journal of Ornithology)*, *19*(2), 97–110. https://doi.org/10.2307/3676458

Helm, B., & Visser, M. E. (2010). Heritable circadian period length in a wild bird population. *Proceedings of the Royal Society B: Biological Sciences*, *277*(1698), 3335–3342. https://doi.org/10.1098/rspb.2010.0871

Helm, B., Visser, M. E., Schwartz, W., Kronfeld-Schor, N., Gerkema, M., Piersma, T., & Bloch, G. (2017). Two sides of a coin: Ecological and chronobiological perspectives of timing in the wild. *Philosophical Transactions of the Royal Society B: Biological Sciences*, *372*(1734), 20160246. https://doi.org/10.1098/rstb.2016.0246

Houslay, T. M., & Wilson, A. J. (2017). Avoiding the misuse of BLUP in behavioural ecology. *Behavioral Ecology: Official Journal of the International Society for Behavioral Ecology*, *28*(4), 948–952. https://doi.org/10.1093/beheco/arx023

Jabbur, M. L., Dani, C., Spoelstra, K., Dodd, A. N., & Johnson, C. H. (2024). Evaluating the Adaptive Fitness of Circadian Clocks and their Evolution. *Journal of Biological Rhythms*, 07487304231219206. https://doi.org/10.1177/07487304231219206

Johnson, C. H., Elliott, J. A., & Foster, R. (2003). Entrainment of Circadian Programs. *Chronobiology International*, *20*(5), 741–774. https://doi.org/10.1081/CBI-120024211

Jonasson, K. A. (2017). *The effects of sex, energy, and environmental conditions on the movement ecology of migratory bats* [The University of Western Ontario]. Electronic Thesis and Dissertation Repository. 4411. https://ir.lib.uwo.ca/etd/4411/

Konopka, R. J., & Benzer, S. (1971). Clock mutants of Drosophila melanogaster. *Proceedings of the National Academy of Sciences*, *68*(9), 2112–2116. https://doi.org/10.1073/pnas.68.9.2112

Krittika, S., & Yadav, P. (2020). Circadian clocks: An overview on its adaptive significance. *Biological Rhythm Research*, *51*(7), 1109–1132. https://doi.org/10.1080/09291016.2019.1581480

Kyriacou, C. P., Peixoto, A. A., Sandrelli, F., Costa, R., & Tauber, E. (2008). Clines in clock genes: Fine-tuning circadian rhythms to the environment. *Trends in Genetics*, *24*(3), 124–132. https://doi.org/10.1016/j.tig.2007.12.003

Laine, V. N., Atema, E., Vlaming, P., Verhagen, I., Mateman, C., Ramakers, J. J. C., van Oers, K., Spoelstra, K., & Visser, M. E. (2019). The Genomics of Circadian Timing in a Wild Bird, the Great Tit (Parus major). *Frontiers in Ecology and Evolution*, *7*. https://www.frontiersin.org/articles/10.3389/fevo.2019.00152

Lehmann, M., Spoelstra, K., Marcel E. Visser, & Helm, B. (2012). Effects of Temperature on Circadian Clock and Chronotype: An Experimental Study on a Passerine Bird. *Chronobiology International*, *29*(8), 1062–1071. https://doi.org/10.3109/07420528.2012.707159

Marimuthu, G. (1984). Seasonal Changes in the Precision of the Circadian Clock of a Tropical Bat under Natural Photoperiod. *Oecologia*, *61*(3), 352–357. https://doi.org/10.1007/BF00379634

Martorell-Barceló, M., Campos-Candela, A., & Alós, J. (2018). Fitness consequences of fish circadian behavioural variation in exploited marine environments. *PeerJ*, *6*, e4814. https://doi.org/10.7717/peerj.4814

Michael, T. P., Salomé, P. A., Yu, H. J., Spencer, T. R., Sharp, E. L., McPeek, M. A., Alonso, J. M., Ecker, J. R., & McClung, C. R. (2003). Enhanced Fitness Conferred by Naturally Occurring Variation in the Circadian Clock. *Science*, *302*(5647), 1049–1053. https://doi.org/10.1126/science.1082971

Mistlberger, R. E. (1994). Circadian food-anticipatory activity: Formal models and physiological mechanisms. *Neuroscience and Biobehavioral Reviews*, *18*(2), 171–195. https://doi.org/10.1016/0149-7634(94)90023-x

Mrosovsky, N. (1999). Masking: History, definitions, and measurement. *Chronobiology International*, *16*(4), 415–429. https://doi.org/10.3109/07420529908998717

Nikhil, K. L., Abhilash, L., & Sharma, V. K. (2016). Molecular Correlates of Circadian Clocks in Fruit Fly *Drosophila melanogaster* Populations Exhibiting early and late Emergence Chronotypes. *Journal of Biological Rhythms*, *31*(2), 125–141. https://doi.org/10.1177/0748730415627933

Nord, A., Lehmann, M., MacLeod, R., McCafferty, D. J., Nager, R. G., Nilsson, J.-Å., & Helm, B. (2016). Evaluation of two methods for minimally invasive peripheral body temperature measurement in birds. *Journal of Avian Biology*, *47*(3), 417–427. https://doi.org/10.1111/jav.00845

Oda, G. A., & Valentinuzzi, V. S. (2023). A clock for all seasons in the subterranean. *Journal of Comparative Physiology A*. https://doi.org/10.1007/s00359-023-01677-z

Pittendrigh, C. S. (1958). Adaptation, natural selection, and behavior. In A. Roe & G. G. Simpson (Eds.), *Behavior and evolution* (p. 416). Yale University Press.

Pittendrigh, C. S. (1960). Circadian rhythms and the circadian organization of living systems. *Cold Spring Harbor Symposia on Quantitative Biology*, *25*, 159–184. https://doi.org/10.1101/sqb.1960.025.01.015

Pittendrigh, C. S., & Daan, S. (1976a). A functional analysis of circadian pacemakers in nocturnal rodents I. The stability and liability of spontaneous frequency. *Journal of Comparative Physiology*, *106*(3), 223–252. https://doi.org/10.1007/BF01417856

Pittendrigh, C. S., & Daan, S. (1976b). A functional analysis of circadian pacemakers in nocturnal rodents IV. Entrainment: Pacemaker as a clock. *Journal of Comparative Physiology*, *106*(3), 291–331. https://doi.org/10.1007/BF01417859

Pittendrigh, C. S., & Daan, S. (1976c). A functional analysis of circadian pacemakers in nocturnal rodents V. Pacemaker Structure: A Clock for All Seasons. *Journal of Comparative Physiology*, *106*(3), 333–355. https://doi.org/10.1007/BF01417860

Pivarciova, L., Vaneckova, H., Provaznik, J., Wu, B. C., Pivarci, M., Peckova, O., Bazalova, O., Cada, S., Kment, P., Kotwica-Rolinska, J., & Dolezel, D. (2016). Unexpected Geographic Variability of the Free Running Period in the Linden Bug Pyrrhocoris apterus. *Journal of Biological Rhythms*, *31*(6), 568–576. https://doi.org/10.1177/0748730416671213

Pohl, H. (1972). Seasonal change in light sensitivity in Carduelis flammea. *Die Naturwissenschaften*, *59*(11), 518. https://doi.org/10.1007/BF00609831

Pohl, H. (1974). Interaction of effects of light, temperature, and season on the circadian period of Carduelis flammea. *Die Naturwissenschaften*, *61*(9), 406–407. https://doi.org/10.1007/BF00622631

Pohl, H. (2000). Circadian control of migratory restlessness and the effects of exogenous melatonin in the brambling, Fringilla montifringilla. *Chronobiology International*, *17*(4), 471–488. https://doi.org/10.1081/cbi-100101058

R Core Team. (2023). *R: A Language and Environment for Statistical Computing* [Computer software]. R Foundation for Statistical Computing.

Roenneberg, T. (2012). What is chronotype? *Sleep and Biological Rhythms*, *10*, 75–76. https://doi.org/10.1111/J.1479-8425.2012.00541.X

Roenneberg, T., Wirz-Justice, A., & Merrow, M. (2003). Life between clocks: Daily temporal patterns of human chronotypes. *Journal of Biological Rhythms*, *18*(1), 80–90. https://doi.org/10.1177/0748730402239679

Rotics, S., Dayan, T., Levy, O., & Kronfeld-Schor, N. (2011). Light masking in the field: An experiment with nocturnal and diurnal spiny mice under semi-natural field conditions. *Chronobiology International*, *28*(1), 70–75. https://doi.org/10.3109/07420528.2010.525674

Royal Netherlands Meteorological Institute (KNMI). (2023). *Daggegevens van het weer in Nederland.* [dataset]. Royal Netherlands Meteorological Institute (KNMI). https://www.knmi.nl/nederland-nu/klimatologie/daggegevens

Salmela, M. J., & Weinig, C. (2019). The fitness benefits of genetic variation in circadian clock regulation. *Current Opinion in Plant Biology*, *49*, 86–93. https://doi.org/10.1016/j.pbi.2019.06.003

Sanders, D., Frago, E., Kehoe, R., Patterson, C., & Gaston, K. J. (2021). A meta-analysis of biological impacts of artificial light at night. *Nature Ecology & Evolution*, *5*(1), Article 1. https://doi.org/10.1038/s41559-020-01322-x

Schmal, C., Herzel, H., & Myung, J. (2020). Clocks in the Wild: Entrainment to Natural Light. *Frontiers in Physiology*, *11*(272), 1–12.

Schmal, C., Myung, J., Herzel, H., & Bordyugov, G. (2015). A Theoretical Study on Seasonality. *Frontiers in Neurology*, *6*. https://www.frontiersin.org/articles/10.3389/fneur.2015.00094

Schwartz, W. J., Helm, B., & Gerkema, M. P. (2017). Wild clocks: Preface and glossary. *Phil. Trans. R. Soc. B*, *372*(1734), 20170211. https://doi.org/10.1098/rstb.2017.0211

SensorGnome Project. (2018). *SensorGnome Project. Raspberry PI Sensorgnome (release 2018-10-12). .* [Computer software]. https://sensorgnome.org/

Shimmura, T., Nakayama, T., Shinomiya, A., Fukamachi, S., Yasugi, M., Watanabe, E., Shimo, T., Senga, T., Nishimura, T., Tanaka, M., Kamei, Y., Naruse, K., & Yoshimura, T. (2017). Dynamic plasticity in phototransduction regulates seasonal changes in color perception. *Nature Communications*, *8*(1), Article 1. https://doi.org/10.1038/s41467-017-00432-8

Spoelstra, K., Verhagen, I., Meijer, D., & Visser, M. E. (2018). Artificial light at night shifts daily activity patterns but not the internal clock in the great tit (*Parus major*). *Proc. R. Soc. B*, *285*(1875), 20172751. https://doi.org/10.1098/rspb.2017.2751

Strauß, A. F. T., Bosma, L., Visser, M. E., & Helm, B. (2024). Short-time exposure to light at night affects incubation patterns and correlates with subsequent body weight in great tits (*Parus major*). *Journal of Experimental Zoology A*.

Strauß, A. F. T., McCafferty, D. J., Nord, A., Lehmann, M., & Helm, B. (2022). Using skin temperature and activity profiles to assign chronotype in birds. *Animal Biotelemetry*, *10*(1), 27. https://doi.org/10.1186/s40317-022-00296-w

Stuber, E. F., Dingemanse, N. J., Kempenaers, B., & Mueller, J. C. (2015). Sources of intraspecific variation in sleep behaviour of wild great tits. *Animal Behaviour*, *106*, 201–221. https://doi.org/10.1016/j.anbehav.2015.05.025

Taylor, P. D., Crewe, T. L., Mackenzie, S. A., Lepage, D., Aubry, Y., Crysler, Z., Finney, G., Francis, C. M., Guglielmo, C. G., Hamilton, D. J., Holberton, R. L., Loring, P. H., Mitchell, G. W., Norris, D. R., Paquet, J., Ronconi, R. A., Smetzer, J. R., Smith, P. A., Welch, L. J., & Woodworth, B. K. (2017). The Motus Wildlife Tracking System: A collaborative

research network to enhance the understanding of wildlife movement. *Avian Conservation and Ecology*, *12*(1), 8. https://doi.org/10.5751/ACE-00953-120108
Tomotani, B. M., Flores, D. E. F. L., Tachinardi, P., Paliza, J. D., Oda, G. A., & Valentinuzzi, V. S. (2012). Field and Laboratory Studies Provide Insights into the Meaning of Day-Time Activity in a Subterranean Rodent (Ctenomys aff. Knighti), the Tuco-Tuco. *PLOS ONE*, *7*(5), e37918. https://doi.org/10.1371/journal.pone.0037918
Tomotani, B. M., Timpen, F., & Spoelstra, K. (2023). Ingrained city rhythms: Flexible activity timing but more persistent circadian pace in urban birds. *Proceedings of the Royal Society B*, *290*(20222605), 1–9. https://doi.org/10.1098/rspb.2022.2605
van der Vinne, V., Riede, S. J., Gorter, J. A., Eijer, W. G., Sellix, M. T., Menaker, M., Daan, S., Pilorz, V., & Hut, R. A. (2014). Cold and hunger induce diurnality in a nocturnal mammal. *Proceedings of the National Academy of Sciences*, *111*(42), 15256–15260. https://doi.org/10.1073/pnas.1413135111
Walton, J. C., Bumgarner, J. R., & Nelson, R. J. (2022). Sex Differences in Circadian Rhythms. *Cold Spring Harbor Perspectives in Biology*, *14*(7), a039107. https://doi.org/10.1101/cshperspect.a039107
Wicht, H., Korf, H.-W., Ackermann, H., Ekhart, D., Fischer, C., & Pfeffer, M. (2014). Chronotypes and rhythm stability in mice. *Chronobiology International*, *31*(1), 27–36. https://doi.org/10.3109/07420528.2013.820739
Wiebe, K. L., Wiehn, J., & Korpimäki, E. (1998). The onset of incubation in birds: Can females control hatching patterns? *Animal Behaviour*, *55*(4), 1043–1052. https://doi.org/10.1006/anbe.1997.0660
Woelfle, M. A., & Johnson, C. H. (2009). The Adaptive Value of the Circadian Clock System in Cyanobacteria. In J. L. Ditty, S. R. Mackey, & C. H. Johnson (Eds.), *Bacterial Circadian Programs* (pp. 205–221). Springer. https://doi.org/10.1007/978-3-540-88431-6_12
Womack, R. J., Capilla-Lasheras, P., McGlade, C. L. O., Dominoni, D. M., & Helm, B. (2023). Reproductive fitness is associated with female chronotype in a songbird. *Animal Behaviour*, *205*, 65–78. https://doi.org/10.1016/j.anbehav.2023.08.018
Zawilska, J. B., Lorenc, A., Berezińska, M., Vivien-Roels, B., Pévet, P., & Skene, D. J. (2006). Diurnal and circadian rhythms in melatonin synthesis in the turkey pineal gland and retina. *General and Comparative Endocrinology*, *145*(2), 162–168. https://doi.org/10.1016/j.ygcen.2005.08.008

SUPPORTING INFORMATION

Additional supporting information can be found online in the Supporting Information section at the end of this article.

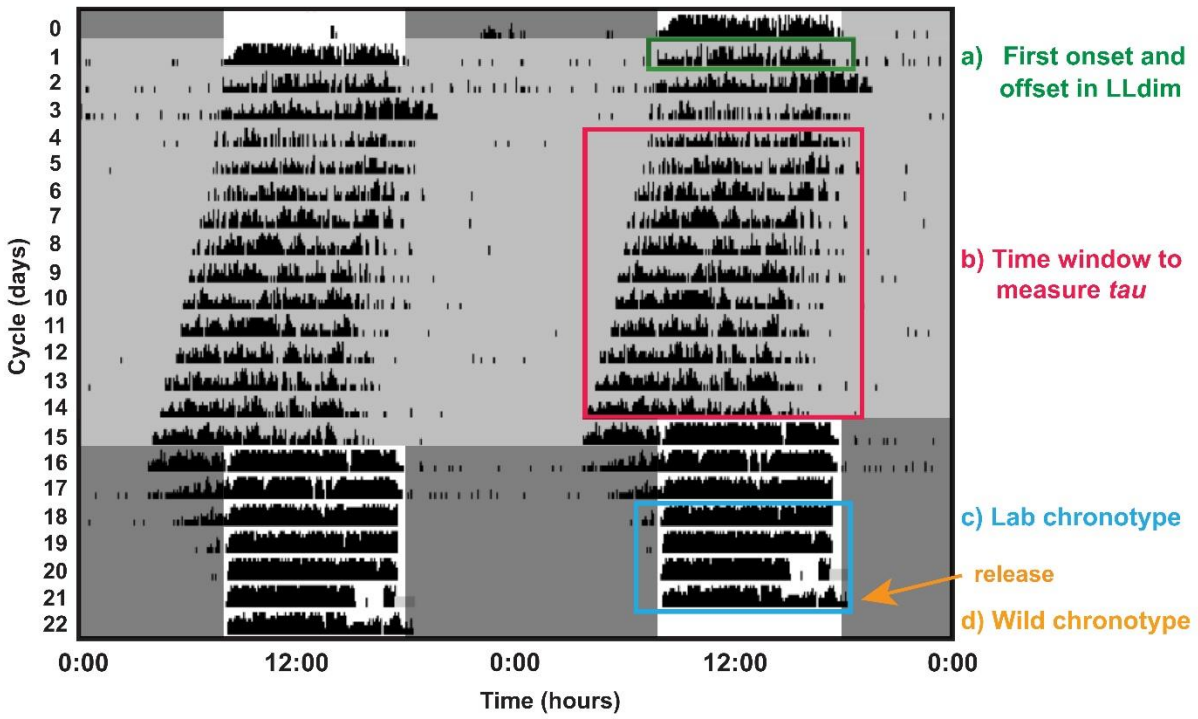

Figure 1. Actogram illustration our experimental design with parts made in the captivity and in the wild.

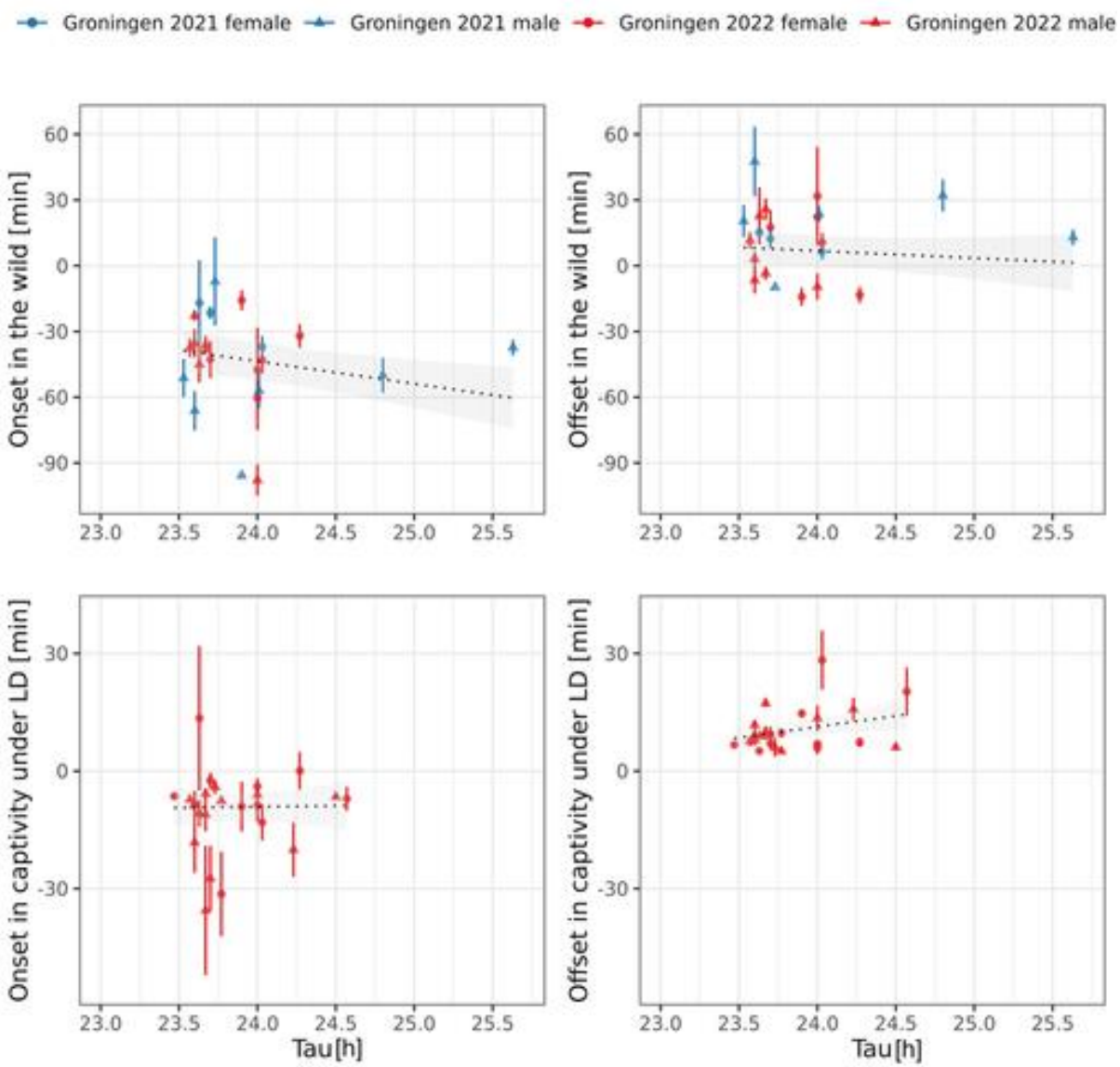

Figure 2. The relationship between tau and activity onset and offset.

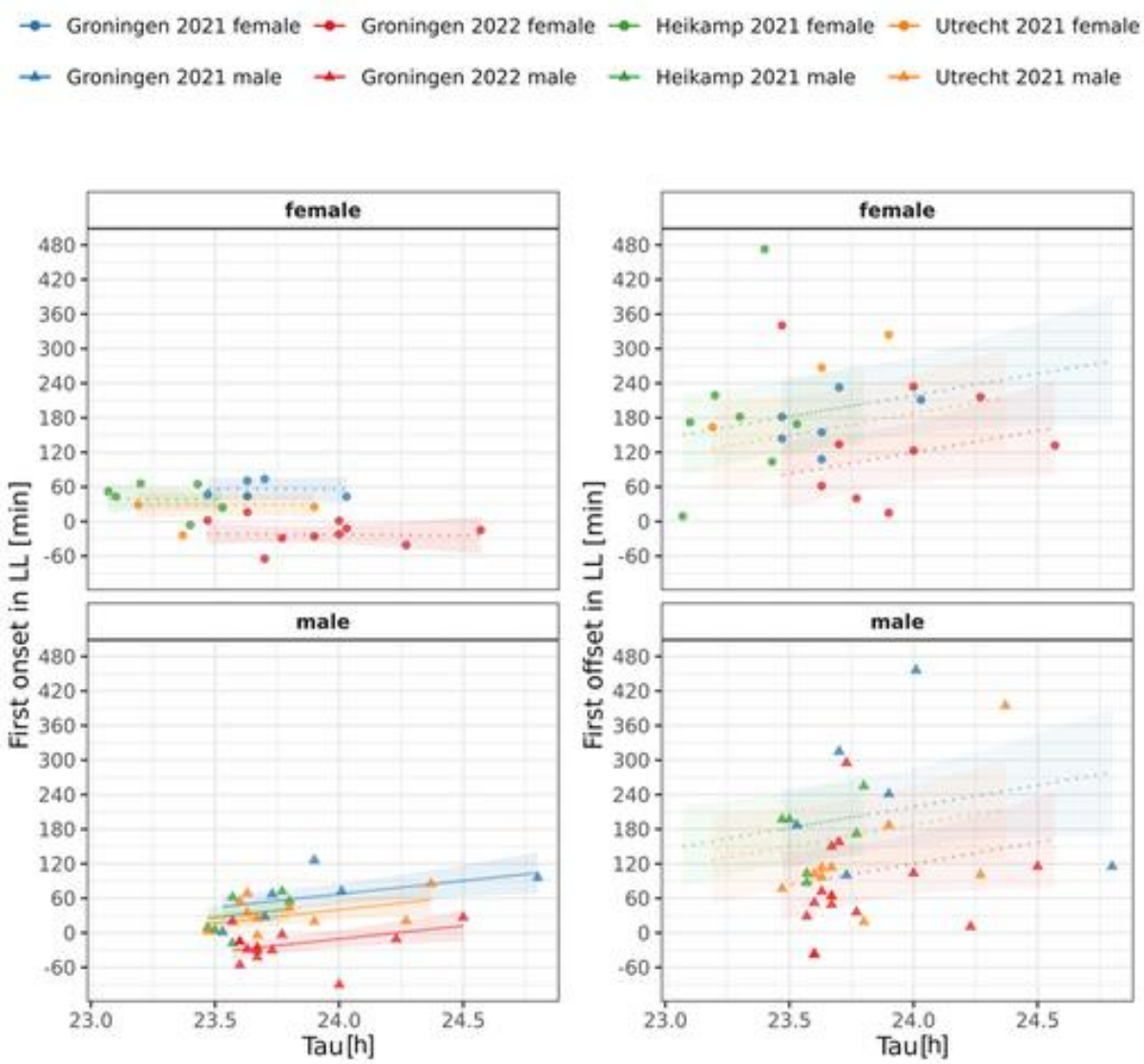

Figure 3. The relationship between the first onset in LL and tau depended on sex.

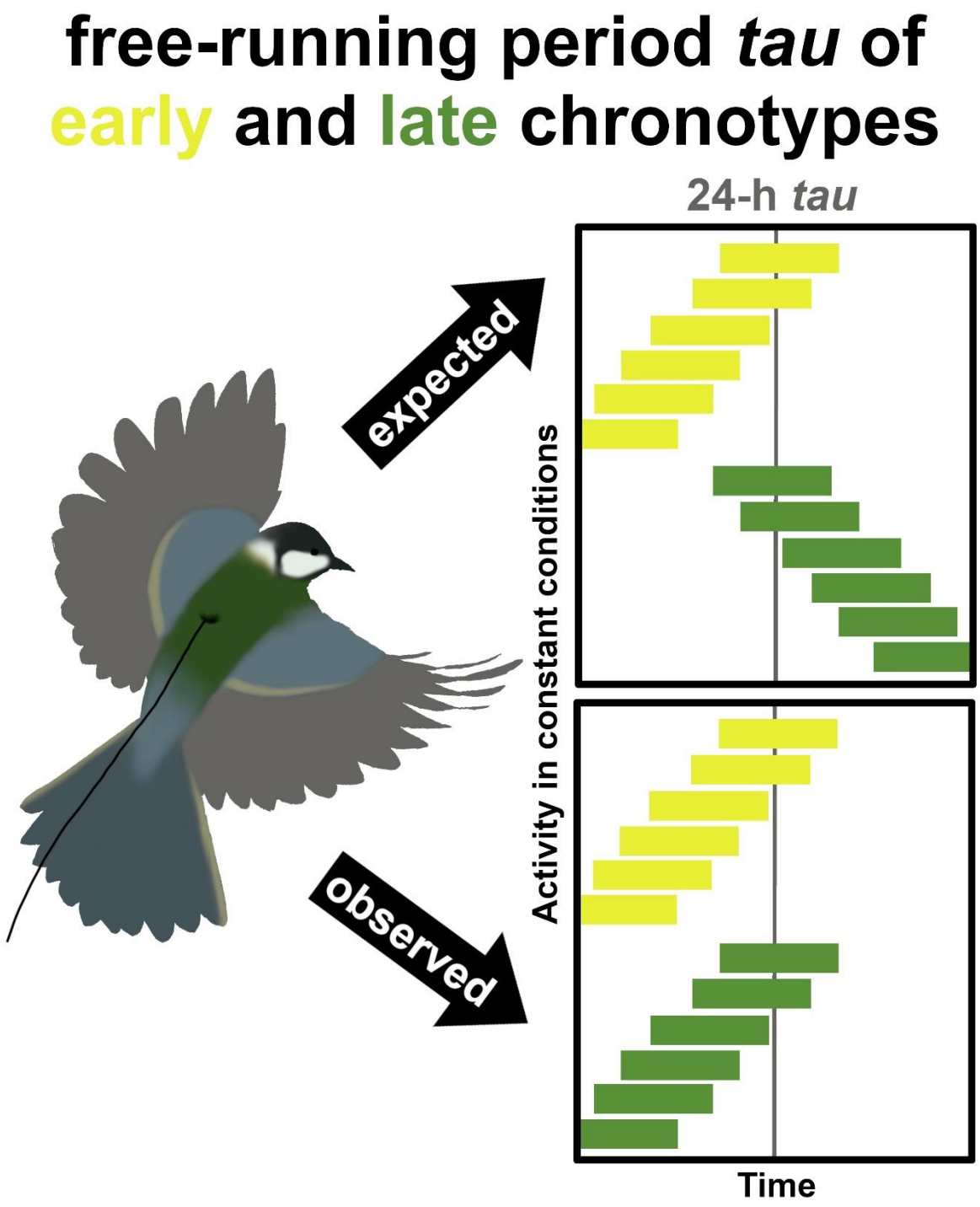

Graphical Abstract:

Wild birds showed chronotypes in the field that were unlinked to their circadian period length tau measured in captivity. In males only, the first onset of activity after exposure to constant dim light did correlate with tau. Our study emphasises the need to investigate clocks in the real world, including a need to better understand masking.

Supporting Information

Circadian clock period length is not consistently linked to chronotype in a wild songbird

Barbara M. Tomotani*, Aurelia F. T. Strauß*, Dmitry Kishkinev, Huib van de Haar and Barbara Helm

** These authors contributed equally to this work.*

2024-07-30

for European Journal of Neuroscience

Table of Content

Part S1: Additional Information on Methods and Results

Sample sizes

Table S1_1: Number of birds for each measurement, numbers differ between measurements due to data loss, insufficient data quality, etc.

	Groningen 2021		Heikamp 2021		Utrecht 2021		Groningen 2022	
Number of birds	**females**	**males**	**females**	**males**	**females**	**males**	**females**	**males**
Tau	6	8	7	6	4	10	10	14
First onset in LL	5	7	6	7	4	10	10	13
First offset in LL	6	7	7	7	3	10	9	14
Lab chronotype onset							10	14
Lab chronotype offset							10	14
Wild chronotype onset	3	7	1	0	2	2	6	7
Wild chronotype offset	3	6	1	0	2	2	6	7
Wild skin temp. min.	3	4	1	0	2	2	6	7

Experimental set-up

Figure S1_1: Photo of the experimental set-up for measuring activity rhythms. We had groups of 6 individual cages with a metal front in stand-alone plywood racks. Cages were separated from one another by wood panels that surrounded them except for the front side. These panels prevented birds from seeing any of their neighbours. The front of the cages was covered by a wooden door that could be opened for feeding and caretaking. Photo by Barbara M. Tomotani.

Light spectral distribution

We measured the spectral composition of the lamps used in the experiment (0.5 lux intensity) using an Ocean Insight OEPro spectrometer. Measurements of absolute irradiance (µW/cm2.nm) collected with a 200 µm slit and standard cosine corrector were input into the online toolbox Alphaopics: Species-specific light exposure calculator (McDowell et al., 2023) to obtain the plot of the spectral power distribution (Figure S1_2) and calculations of total irradiance, total photon and photopic illuminance. Because there are no great tit-specific photoreceptor data and other birds were absent from the list, we report here the calculations for humans:

Total irradiance [W/m^2]: 0.0007

Total photon [$log(photons/cm^2/s)$]: 11.3007

Human photopic illuminance [lux]: 0.2697

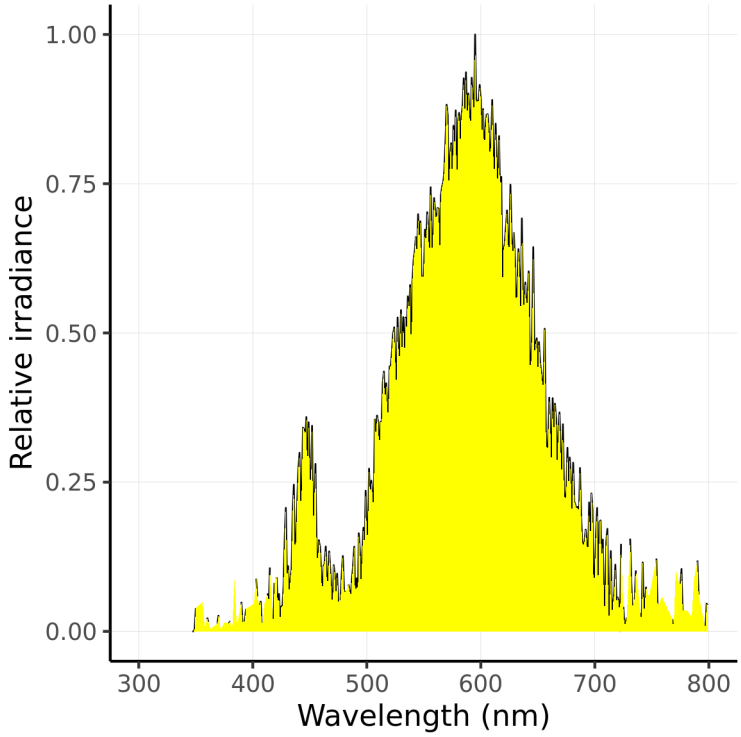

Figure S1_2: Plot of spectral power distribution (W/m^2.nm).

Actograms showing activity patterns under dim light (LL) and light-dark (LD) conditions in the lab

Figure S1_3: Double-plotted actograms of males from Groningen (2021). For all actograms, see explanations of the conditions experienced by the birds in Figure 1 of the main manuscript.

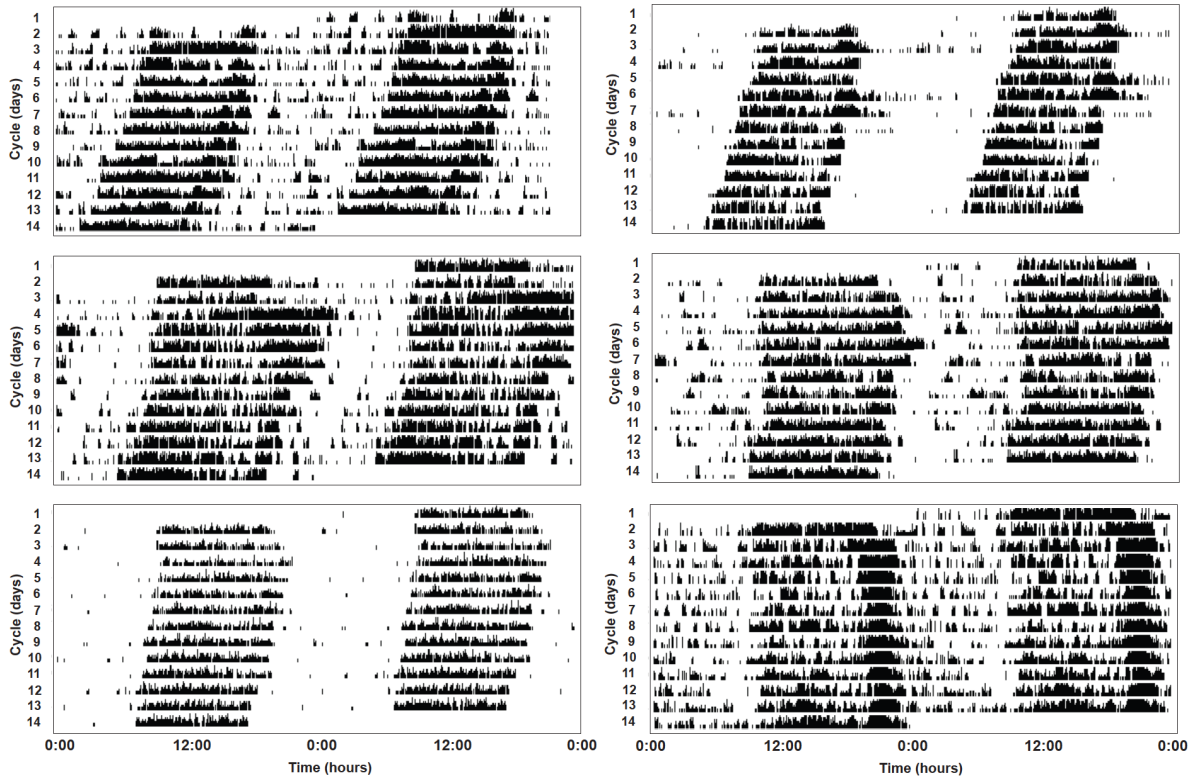

Figure S1_4: Double-plotted actograms of females from Groningen (2021)

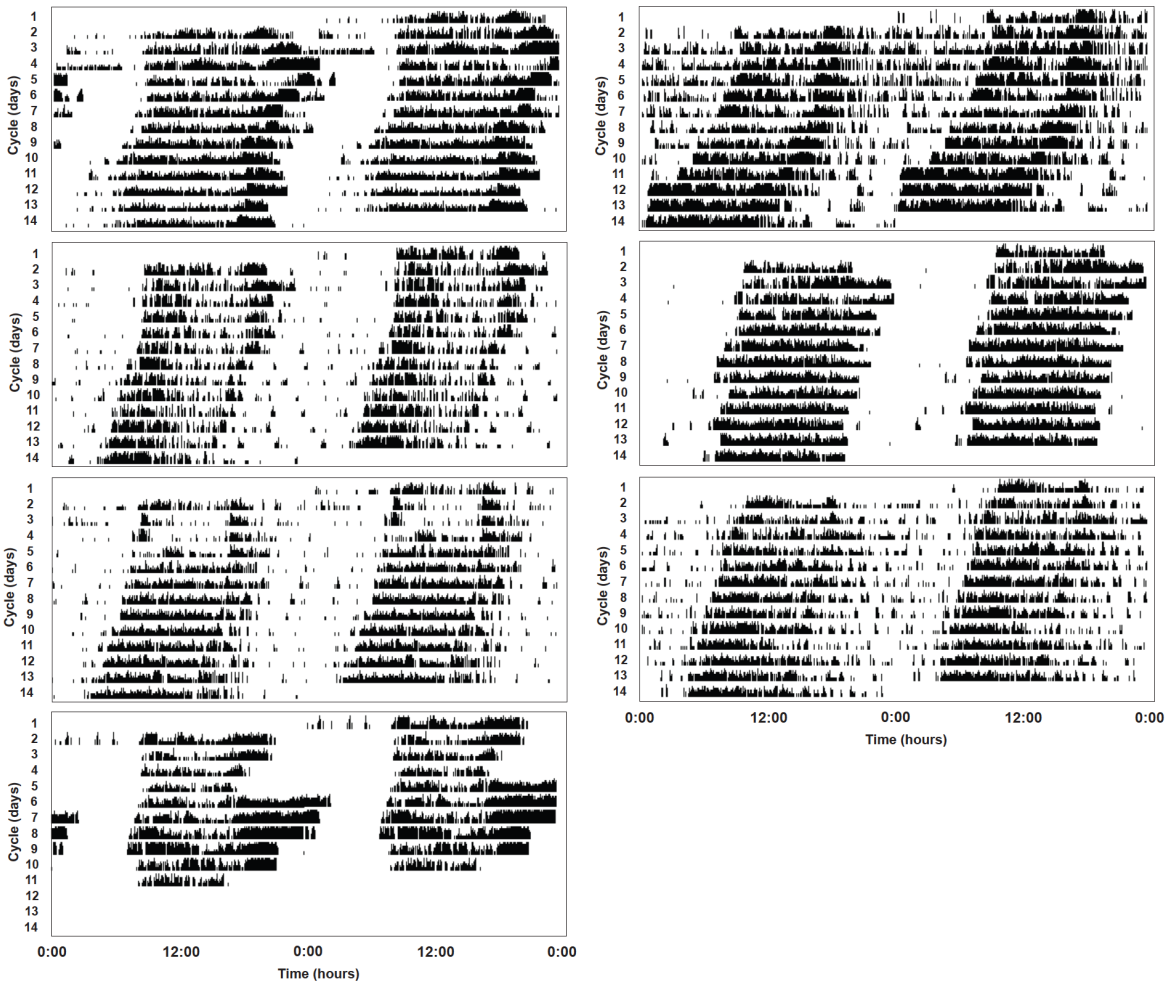

Figure S1_5: Double-plotted actograms of males from Heikamp (2021)

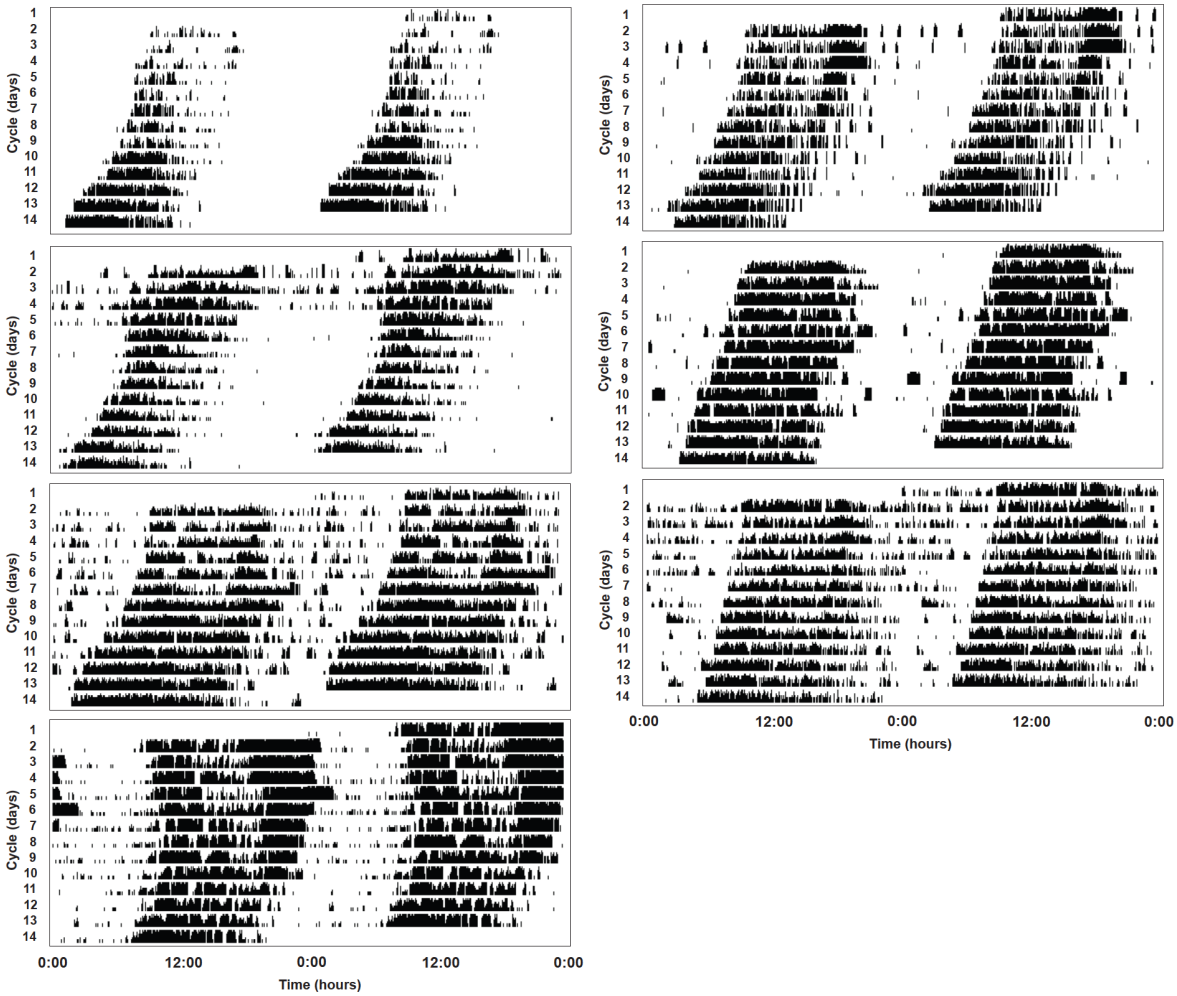

Figure S1_6: Double-plotted actograms of females from Heikamp (2021)

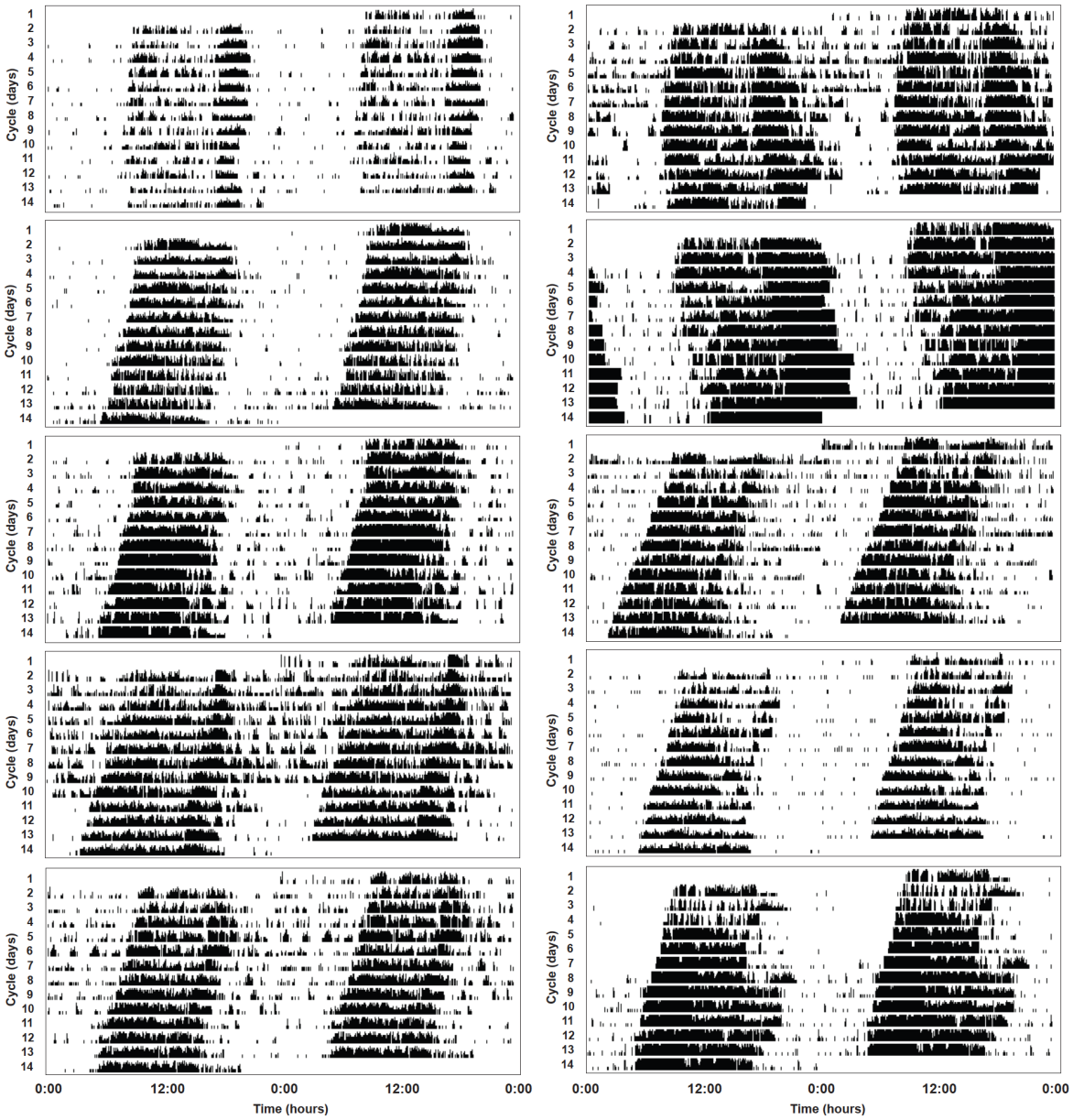

Figure S1_7: Double-plotted actograms of males from Utrecht (2021)

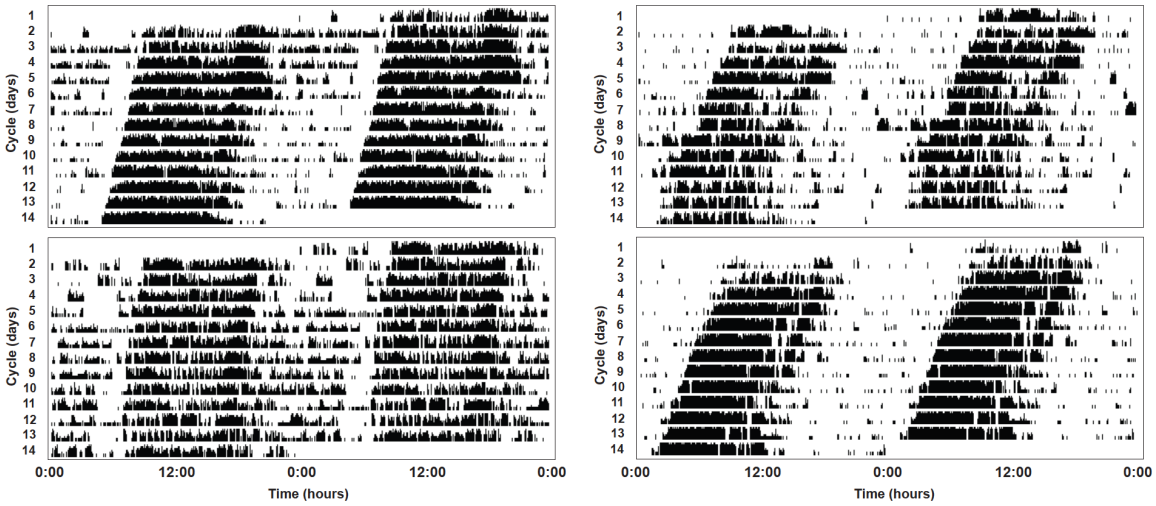

Figure S1_8: Double-plotted actograms of females from Utrecht (2021)

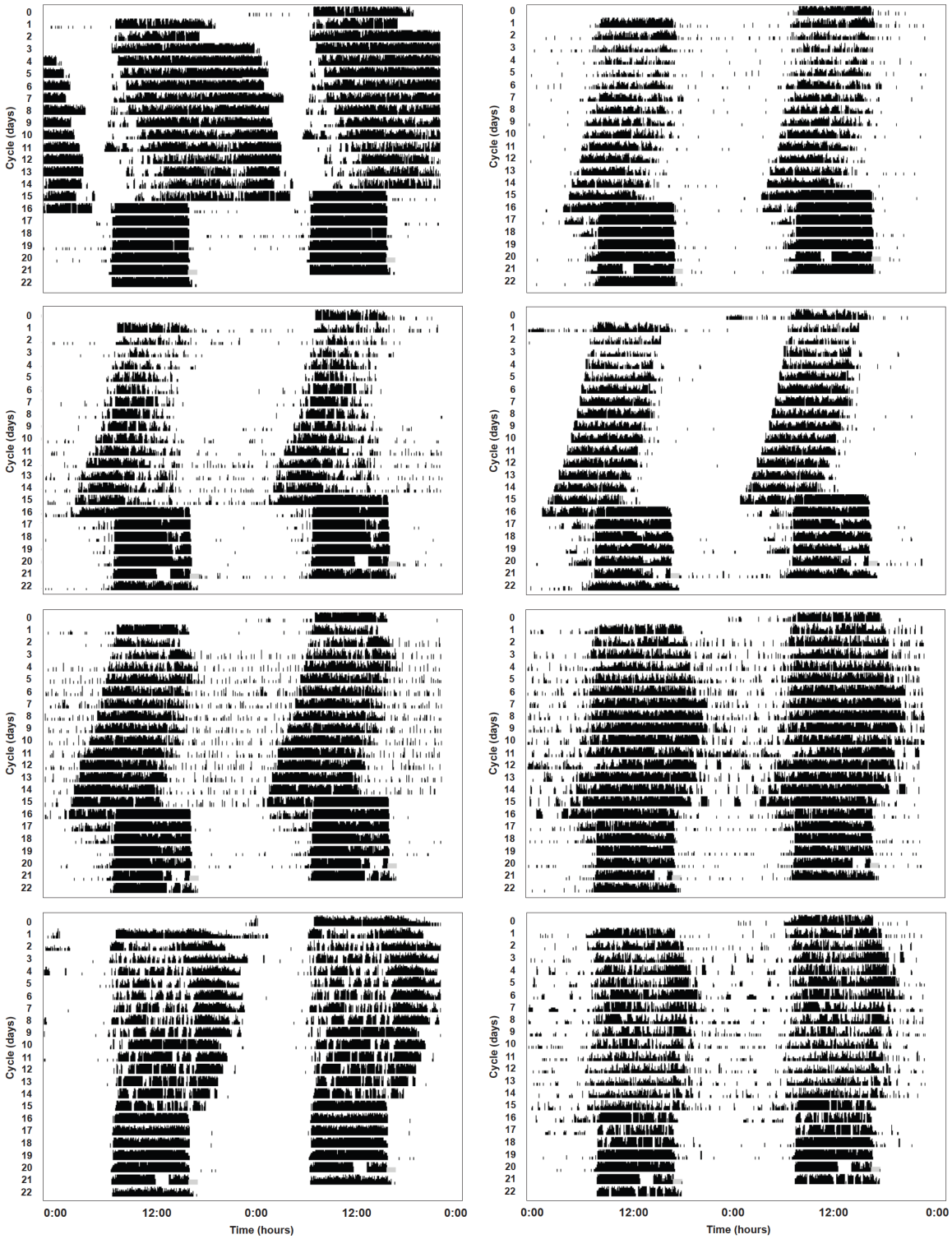

Figure S1_9: Double-plotted actograms of males from Groningen (2022)

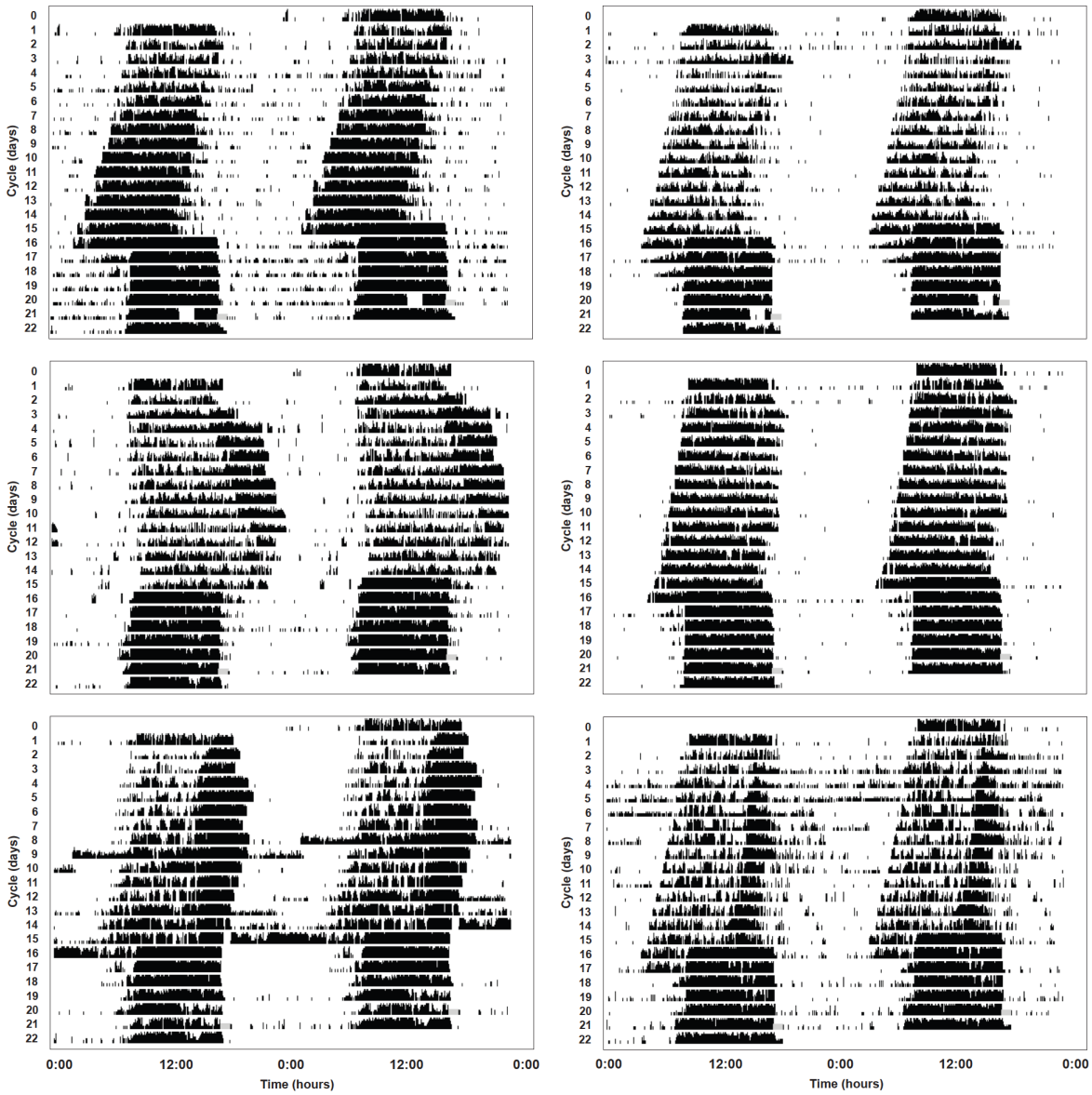

Figure S1_9 (cont.): Double-plotted actograms of males from Groningen (2022)

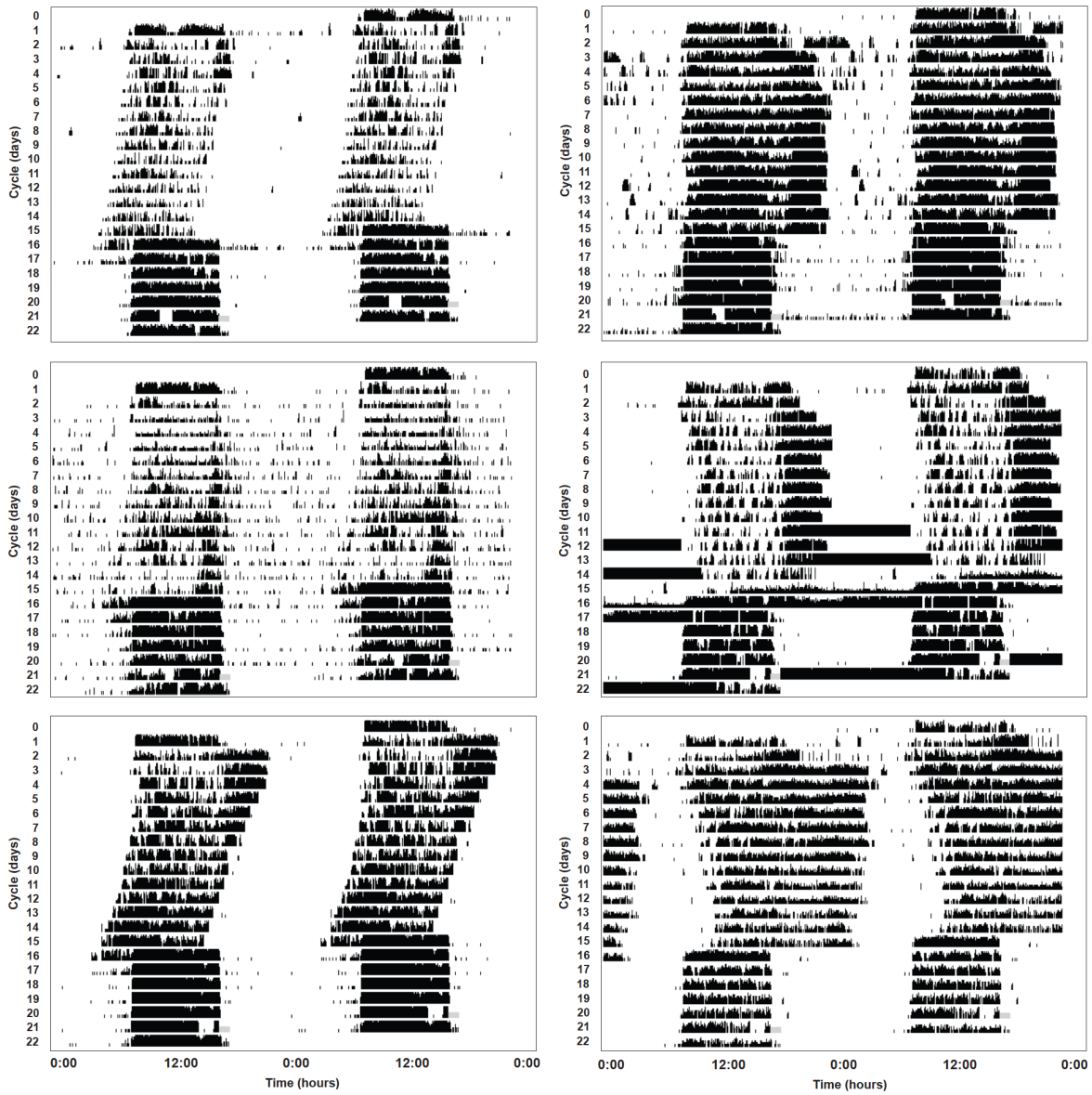

Figure S1_10: Double-plotted actograms of females from Groningen (2022)

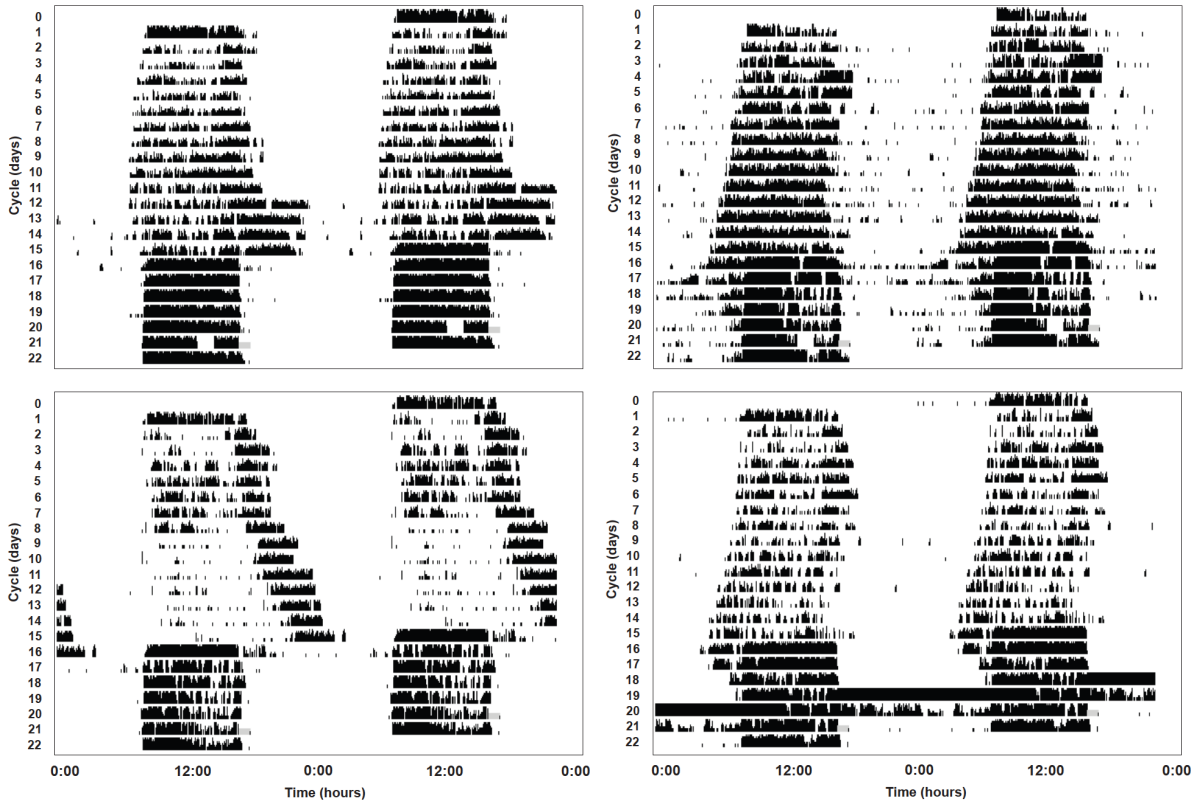

Figure S1_10 (cont.): Double-plotted actograms of females from Groningen (2022)

Variation and factors influencing the length of the free-running period (t*au*)

In this study, *tau* was normally distributed around a mean of 23.75 ± 0.04 h, and differed between the bird groups tested (Figure S1_11 & Table S1_2).

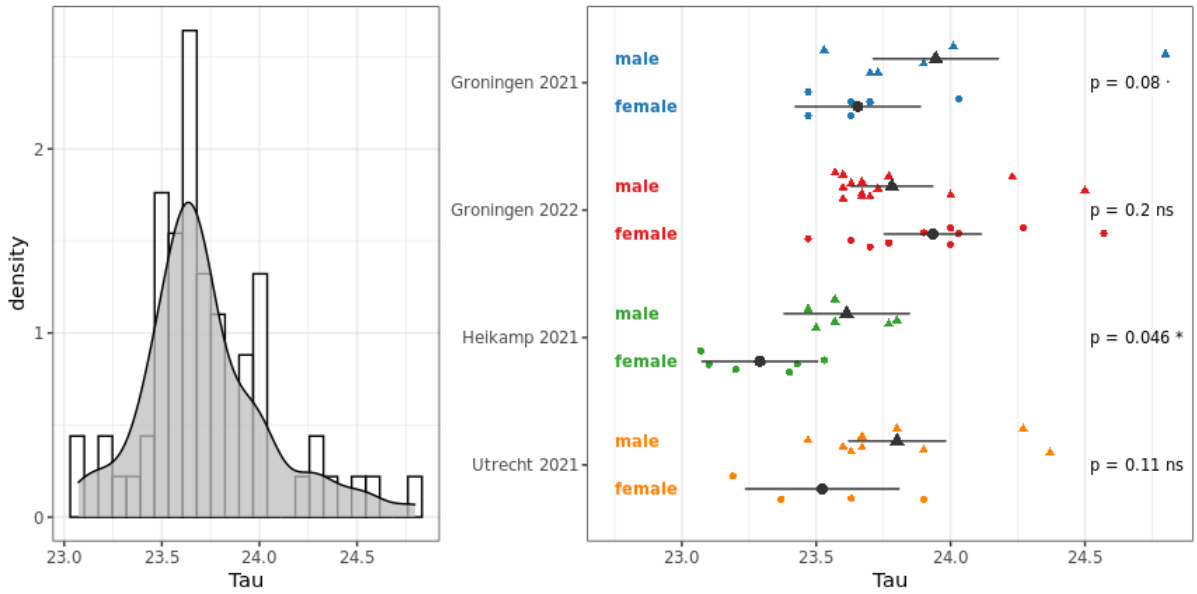

Figure S1_11: Tau [h] during constant dim light (LL) of 63 individuals in this study. Left) Distribution of tau. Right) Tau per group and sex (colours indicate groups, triangles stand for males, circles for females); significance levels derive from pairwise comparisons of the sexes within group using the *emmeans* package (Lenth 2023).

Table S1_2: Test statistics and estimates for tau [h] across groups (Gro22, Groningen 2022, Gro21 = Groningen 2021, Utr21 = Utrecht 2021, Hei21 = Heikamp 2021) and sexes (f = female, m = male). Statistics were obtained by stepwise model reduction and estimates for the model with all non-significant interactions dropped. "X^2" refers to Chi-square. In a post hoc tests using the *emmeans* package (Lenth 2023) sex were compared within group.

		***Tau* n = 63**					***Post hoc***			**female – male**	
	df	**F**	**p**		**Estimate**	**SE**		**t ratio**	**p**	**Estimate**	**SE**
Intercept (f)				Gro21	23.66	0.12	Gro21	-1.76	0.08	-0.29	0.17
Group	3			Gro22	0.28	0.15	Gro22	1.29	0.20	0.15	0.12
				Hei21	-0.37	0.16	Hei21	-2.03	0.046 *	-0.32	0.16
				Utr21	-0.13	0.18	Utr21	-1.65	0.11	-0.28	0.17
Sex (m)	1				0.29	0.17					
Group*Sex	3	2.96	0.04 *	Gro22	-0.44	0.20					
				Hei21	0.03	0.23					
				Utr21	-0.01	0.24					
		X^2	**p**		**Var**	**SD**					
Rack n=7	1	0.00	1.00		0.00	0.00					
Residual					0.09	0.30					

Change in the timing of onset during exposure to constant dim light (LL)

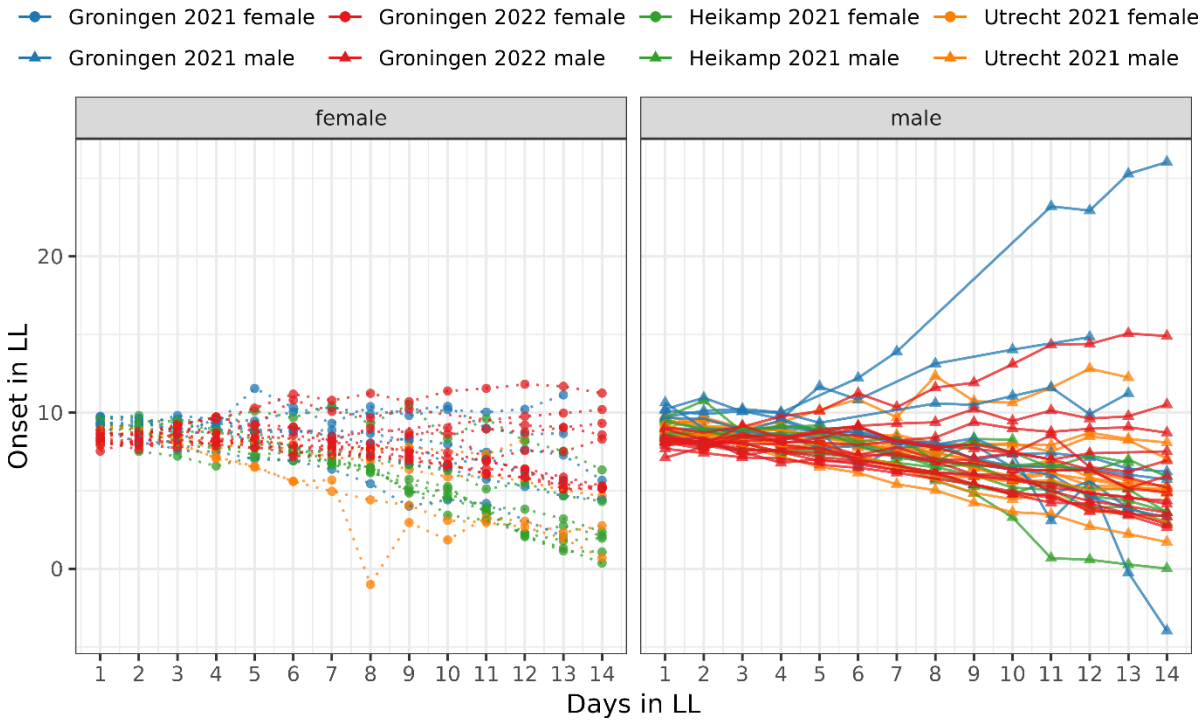

Figure S1_12: Change over time in the onsets of activity (h, clock time CET) after transferring birds to constant dim light (LL) in the lab, revealing the day-to-day changes in clock period.

Wild chronotype - activity

Table S1_3: Test statistics and estimates for activity onset or offset in the wild after release, relative to sunrise or sunset [min], respectively. "Phase in LL" refers to first onset and offset in LL, respectively. Statistics were obtained by stepwise model reduction and estimates for the model with all non-significant interactions dropped. (Groups: Gro22, Groningen 2022, Gro21 = Groningen 2021; and sexes: f = female, m = male.).

Activity		**Onset in the wild n = 223**				**Offset in the wild n = 178**			
	df	**F**	**p**	**Estimate**	**SE**	**F**	**p**	**Estimate**	**SE**
Intercept (Gro21, f)				209	209			34	174
Tau [h]	1	1.45	0.25	-11	9	0.00	0.98	0	7
Phase in LL [min]	1	3.08	0.10	0	0	0.20	0.66	0	0
Group (Gro22)	1	1.15	0.30	16	15	0.11	0.75	-3	9
Sex (m)	1	2.53	0.14	-13	8	0.37	0.55	4	7
Julian day	1	0.01	0.91	0	0	5.19	0.02 *	-1	0
Mean Temp. (n/d)	1	0.25	0.62	0	0	1.45	0.23	-1	0
*Tau**Group (Gro22)	1	2.92	0.11			3.25	0.10 .		
*Tau**Sex (m)	1	0.04	0.85			0.00	0.98		
Phase*Group (Gro22)	1	1.83	0.20			1.13	0.31		
Phase*Sex (m)	1	0.00	0.97			0.03	0.87		
		X^2	**p**	**Var**	**SD**	X^2	**p**	**Var**	**SD**
Individual n=22|n=20	1	23.30	1e-6 ***	253	16	14.74	1e-4 ***	155	12
Residual				493	22			336	18

Lab chronotype

Table S1_4: Test statistics and estimates for onset or offset in captivity under light-dark (LD) conditions relative to sunrise or sunset [min], respectively. "Phase in LL" refers to first onset and offset in LL, respectively. Statistics were obtained by stepwise model reduction and estimates for the model with all non-significant interactions dropped. "X^2" refers to Chi-square. Sexes: f = female, m = male.

Activity		**Onset in captivity n = 119**				**Offset in captivity n = 111**			
	df	**F**	**p**	**Estimate**	**SE**	**F**	**p**	**Estimate**	**SE**
Intercept (f)				36	159			-108	69
Tau [h]	1	0.07	0.80	-2	7	3.01	0.10 .	5	3
Phase in LL [min]	1	0.15	0.71	2	4	1.50	0.24	-1	1
Sex (m)	1	0.96	0.34	-4	4	0.07	0.79	0	2
*Tau**Sex (m)	1	0.03	0.86			1.83	0.19		
Phase*Sex (m)	1	0.06	0.82			0.18	0.67		
		X^2	**p**	**Var**	**SD**	X^2	**p**	**Var**	**SD**
Individual n=23	1	8.53	0.004 *	60	8	19.92	8e-6 ***	12	3
Date n=7|n=5	1	2.76	0.10 .	23	5	3.29	0.07 .	2	1
Residual				114	11			16	4

Comparison wild and lab chronotypes

Table S1_5: Test statistics and estimates for activity onset or offset in the wild after release, relative to sunrise or sunset [min], respectively, using only birds that also had a lab chronotype value. Statistics were obtained by stepwise model reduction and estimates for the model with all non-significant interactions dropped. (Groups: Gro22, Groningen 2022; sexes: f = female, m = male; and daytime: n = night for onset, d = day for offset).

Wild vs Lab Gro22		**Onset in the wild n = 143**				**Offset in the wild n = 125**			
	df	**F**	**p**	**Estimate**	**SE**	**F**	**p**	**Estimate**	**SE**
Intercept (f)				-47	22			66	20
Lab Chronotype [min]	1	0.30	0.60	-1	2	0.13	0.73	0	1
Sex (m)	1	0.36	0.56	-8	13	0.02	0.89	1	9
Julian day	1	0.01	0.92	0	0	7.85	0.01 **	-1	0
Mean Temp. (n|d) [°C]	1	0.69	0.41	1	1	2.34	0.13	-2	1
Lab*Sex (m)	1	0.75	0.41			0.70	0.43		
		X^2	**p**	**Var**	**SD**	X^2	**p**	**Var**	**SD**
Individual n=13	1	57.90	3e-14 ***	429	21	20.1	7e-6 ***	202	14
Residual				484	22			362	19

First onset and offset under constant dim light (LL)

Table S1_6: Test statistics and estimates for first onset or offset in constant dim light (LL) relative to expected sunrise or sunset [min], respectively. Statistics were obtained by stepwise model reduction and estimates for the model with all non-significant interactions dropped. (Groups: Gro22, Groningen 2022, Gro21 = Groningen 2021, Utr21 = Utrecht 2021, Hei21 = Heikamp 2021; and sexes: f = female, m = male.)

		Onset in LL n = 60					**Offset in LL n = 61**				
	df	**F**	**p**		**Estimate**	**SE**	**F**	**p**		**Estimate**	**SE**
Intercept (f)				Gro21	109	428			Gro21	-1556	1065
Tau [h]	1				-2	18	2.79	0.10		78	45
Sex (m)	1				-1143	555	2.96	0.09 .		-47	28
Group	3	21.48	3e-9 ***	Gro22	-78	11	3.62	0.02 *	Gro22	-99	36
				Hei21	-18	13			Hei21	1	44
				Utr21	-27	12			Utr21	-32	41
*Tau**Sex (m)	1	4.23	0.04 *		48	23	0.03	0.85			
*Tau**Group	3	0.22	0.88				0.84	0.48			

Table S1_7: Post hoc testing for the first onset in constant dim light (LL) relative to sunrise [min] separately for both sexes. Statistics were obtained by stepwise model reduction. (Groups: Gro22, Groningen 2022, Gro21 = Groningen 2021, Utr21 = Utrecht 2021, Hei21 = Heikamp 2021; and sexes: f = female, m = male.)

Post hoc		**Female n = 25**					**Male n = 35**				
Onset in LL	**df**	**F**	**p**		**Estimate**	**SE**	**F**	**p**		**Estimate**	**SE**
Intercept				Gro21	295	465			Gro21	-1015	442
Tau [h]	1	0.27	0.61		-10	20	5.98	0.02 *		45	18
Group	3	8.77	6e-4 ***	Gro22	-72	14	12.48	2e-5 ***	Gro22	-81	16
				Hei21	-19	17			Hei21	-19	19
				Utr21	-39	17			Utr21	-23	16

Wild chronotype – skin temperature

Table S1_8: Test statistics and estimates for timing of the skin temperature minimum in the wild after release, relative to sunrise [min]. "Phase in LL" refers to first onset and offset in LL, respectively. Statistics were obtained by stepwise model reduction and estimates for the model with all non-significant interactions dropped. (Groups: Gro22, Groningen 2022, Gro21 = Groningen 2021; and sexes: f = female, m = male.)

Skin temperature		**Timing of minima n = 159**			
	df	**F**	**p**	**Estimate**	**SE**
Intercept (Gro21, f)				163	373
Tau [h]	1	2.13	0.20	-23	16
Phase in LL [min]	1	4.83	0.10 .	1	0
Group (Gro22)	1	0.54	0.49	25	34
Sex (m)	1	1.47	0.28	18	15
Julian day	1	0.93	0.34	1	1
Mean Night Temp. [°C]	1	0.12	0.73	1	2
*Tau**Group (Gro22)	1	0.60	0.46		
*Tau**Sex (m)	1	1.20	0.31		
Phase*Group (Gro22)	1	2.43	0.16		
Phase*Sex (m)	1	1.75	0.20		
		X^2	**p**	**Var**	**SD**
Individual n=19	1	0.00	1.00	148	12
Residual				6041	78

Wild vs Lab Gro22		**Timing of minima n = 120**			
	df	**F**	**p**	**Estimate**	**SE**
Intercept (f)				-374	63
Lab Chronotype [min]	1	0.97	0.37	-3	3
Sex (m)	1	0.27	0.62	11	20
Julian day	1	0.41	0.53	1	1
Mean Night Temp. [°C]	1	0.11	0.74	1	2
Lab*Sex (m)	1	1.57	0.26		
		X^2	**p**	**Var**	**SD**
Individual n=13	1	0.26	0.61	540	23
Residual				5307	73

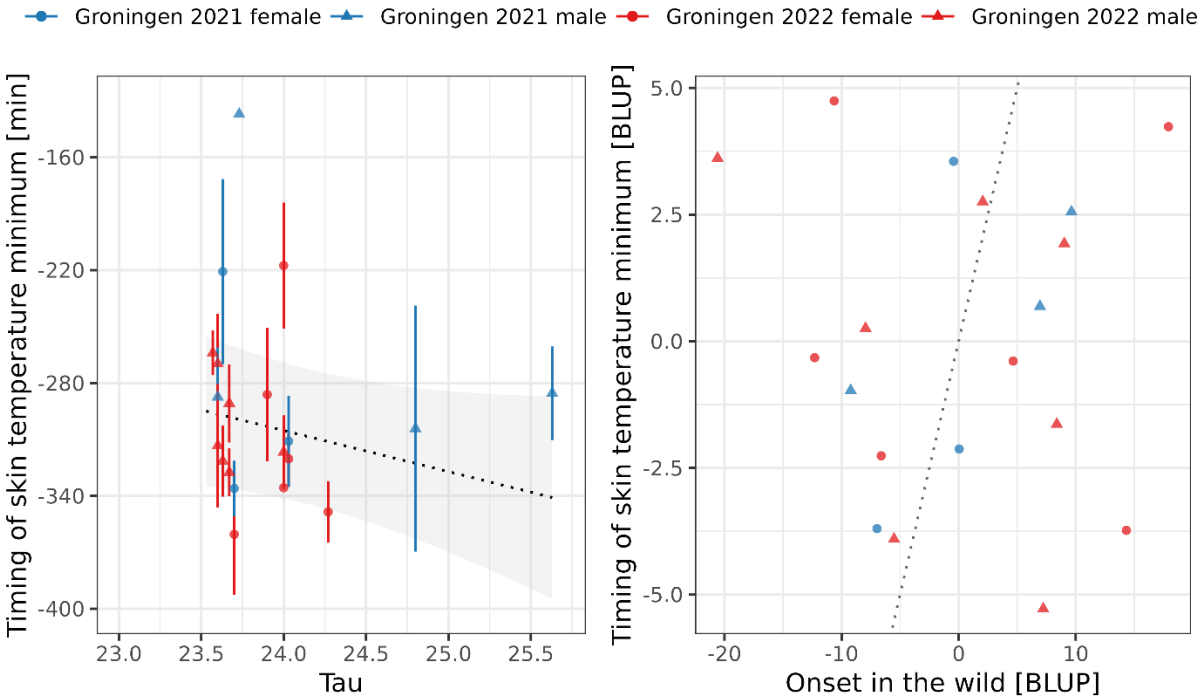

Figure S1_13: Timing of the skin temperature minimum relative to sunrise in the wild after release for 19 individuals: Left) Time of temperature minimum against tau. Right) Time of temperature minimum against activity onset. No significant correlation was detected, using correlation of the residuals (best linear unbiased predictor, BLUP). This type of data was only analysed for Groningen, and thus only for Groningen 2021 and 2022. Colours indicate groups, triangles stand for males, circles for females.

References

Lenth, R. V. (2023). *emmeans*: Estimated Marginal Means, aka Least-Squares Means (version 1.8.8). https://rdocumentation.org/packages/emmeans/versions/1.8.8

McDowell, R. J., Didikoglu, A., Woelders, T., Gatt, M. J., Hut, R. A., Brown, T. M., & Lucas, R. J. (2023). Beyond Lux: Methods for Species and Photoreceptor-Specific Quantification of Ambient Light for Mammals (p. 2023.08.25.554794). bioRxiv. https://doi.org/10.1101/2023.08.25.554794

Part S2: Processing Pipeline for Telemetry Data

Table of Content

1. Telemetry Receiver Settings

For data collection we used the SensorGnome (SG) system based on a freely available software (2023, https://github.com/sensorgnome-org) uploaded to a Raspberry Pi (Model 3B, 2023, https://www.raspberrypi.com/products/raspberry-pi-3-model-b/). The settings (file deployment.txt, see below) were adjusted so that the receiver scanned through a set of deployed frequencies (= one per transmitter) resulting in intervals of 1.5 - 2.8 min depending on the number of frequencies used. The frequencies ranged from 150 to 151 MHz and were spread across the areas to maximise spacing between frequencies of one area (spacing: 0.007 - 0.384 MHz). We set the dongle (FunCube Pro+, 2023, https://www.funcubedongle.com/) to switch the frequency periodically every 10 seconds for all antennas simultaneously, and adjusted two filtering settings, i.e. pulse length to maximal 20 or 25 ms and signal-to-noise ratio (SNR) to minimal 3dB.

```
#### 1. Telemetry Receiver Settings ####
# extract of the adjusted deployment.txt file
{
  "key": {
    "port": ".*",
    "devType": "funcubeProPlus"
    },
  "rate": 48000,
  "channels": 2,
  "schedule": {
    "type": "AlwaysOn"
    },
  "devParams": [
    {
      "name": "frequency",
      "schedule": {
        "type": "periodic",                        # changing frequencies
        "states": [150.020,150.118,150.142...], # frequencies: set as -4 kHz from
                                                     actual frequency
        "periods": [10,10,10,...]                  # period length for frequencies
        }
      },
    ...                                            # other default settings
```

```
  ],
"raw": {
  "enabled": false,
  "chunkMinutes": 0.5
  },
"plugins": [
  {
    "library": "lotek-plugins.so",
    "name": "findpulsefdbatch",
    "outputID": "pulses",
    "params": [
      {
        "name": "plen",                          # filter for max pulse length
        "value": 25                              # 20 ms in 2021, 25 ms in 2022
        },
      {
        "name": "minfreq",                       # min freq deviation: default
        "value": 2
        },
      {
        "name": "maxfreq",                       # max freq deviation: default
        "value": 8
        },
      {
        "name": "fftsize",                       # default
        "value": 24
        },
      {
        "name": "minsnr",                        # filter for min SNR
        "value": 3                               # 3dB to increase range
        },
      {
        "name": "noisesize",                     # default
        "value": 5
        },
      {
        "name": "pulsesep",                      # default
        "value": 1
        }
      ]
    }
  ]
}
```

2. Data Preparation

```
# packages
library(dplyr)      # data management
library(tidyr)
library(reshape2)
library(pracma)     # hampel function
library(diptest)    # data distributions
library(mclust)
library(chron)      # time conversion
library(suncalc)    # sunrise and sunset

options(digits=15)  # increase the numbers of digits available in R to avoid rounding
                      of numeric timestamp
memory.limit(24000) # increase memory limit used to conduct R; usually about 8000

# directories
directory <- "~/R/WinterTelemetry/Data_Telemetry/"
setwd(directory)

file_directory <- "~/R/RawData/Telemetry/"
```

The raw data (separate *txt.gz* files for different dates) from the SGs were merged and produced the following raw data file (Tab. 2.1 columns 1 [Info] to 6 [V6]) with added and disentangled information (Tab. 2.1 columns 7 [Site] to 15 [SNR, signal-to-noise ratio]).

```
#### 2. Data Preparation ####
# get a list of all .gz files names from the file directory including sub-folders
file_list <- list.files(path = file_directory, pattern = "*.gz", recursive = TRUE)

#### 2.1. Data Merging ####
rm(dataset) # remove dataset so that the merging starts anew

# go through file list, name by name
for(a in c(1:length(file_list))){
  file <- file_list[[a]]                    # extract file name
  file2 <- paste(file_directory,file,sep="") # create file path

  # extract info from the file path: e.g. site or receiver
  # (here, equivalent to the names of sub-folders)
  info <- unlist(strsplit(file,split="/"))   # split path
  site <- info[1]                           # extract folder names that are relevant
  receiver <- info[2]

  # if the merged dataset doesn't exist, create it
  if (!exists("dataset")){
    # read in file
    dataset <- read.csv(file2,colClasses=c("character"), header=FALSE)

    # add NA columns if necessary, delete last column if necessary, add info
    ifelse(ncol(dataset)==4,dataset$V5 <-NA,dataset$V5)
    ifelse(ncol(dataset)==5,dataset$V6 <-NA,dataset$V6)
    dataset$V7 <- NULL                       # delete last column if necessary
    dataset$Site <- as.character(paste(site))
    dataset$Receiver <- as.character(paste(receiver))
```

```
  }
  # if the merged dataset does exist, add to it
  if (exists("dataset")){
    # if tryCatch finds an error message, it exchanges the txt.gz file name into a
      txt file*
    temp_dataset <- tryCatch(read.csv(file2,colClasses=c("character"),
header=FALSE),error=function(txt){
      read.csv(gsub(pattern = "\\.gz$", "", file2),colClasses=c("character"),
header=FALSE)})

    # add NA columns if necessary, delete last column if necessary, add info
    ifelse(ncol(temp_dataset)==4,temp_dataset$V5 <-NA,temp_dataset$V5)
    ifelse(ncol(temp_dataset)==5,temp_dataset$V6 <-NA,temp_dataset$V6)
    temp_dataset$V7 <- NULL                  # delete last column if necessary
    temp_dataset$Site <- as.character(paste(site))
    temp_dataset$Receiver <- as.character(paste(receiver))
    dataset<-rbind(dataset, temp_dataset)    # merge the data
    rm(temp_dataset)                         # remove the temporary dataset
  }
}

#### 2.2 Data Extraction ####
dataset <- dataset[!duplicated(dataset), ]   # remove duplicates


# rename and adjust column types
colnames(dataset) <- c("Info","TS_num",paste("V",3:6,sep=""), "Site", "Receiver")
dataset$Info <- as.factor(dataset$Info)
dataset$TS_num <- as.numeric(dataset$TS_num)

# "cleaning" dataset by separating information
dataset$Antenna <- as.factor(NA)             # create new columns
dataset$dfreq <- as.numeric(NA)
dataset$Setting <- as.factor(NA)
dataset$Signal <- as.numeric(NA)
dataset$Setting_Value <- as.numeric(NA)
dataset$BG <- as.numeric(NA)

# assign information from either setting ("S") or detection ("p") row
      # setting rows
dataset$Antenna <- ifelse(dataset$Info=="S",paste("p",dataset$V3,sep=""),NA)
      # detection rows
dataset$Antenna <- as.factor(ifelse(grepl("p", dataset$Info)==TRUE,
      paste(dataset$Info),dataset$Antenna))
dataset$dfreq <- as.numeric(ifelse(grepl("p", dataset$Info)==TRUE,
      paste(dataset$V3),dataset$dfreq))
dataset$Setting <- as.factor(ifelse(dataset$Info=="S",
      paste(dataset$V4),dataset$Setting))
dataset$Signal <- as.numeric(ifelse(grepl("p", dataset$Info)==TRUE,
      paste(dataset$V4),dataset$Signal))
dataset$Setting_Value <- as.numeric(ifelse(dataset$Info=="S",
      paste(dataset$V5),dataset$Setting_Value))
dataset$BG <- as.numeric(ifelse(grepl("p", dataset$Info)==TRUE,
      paste(dataset$V5),dataset$BG))
```

```
dataset$SNR <- as.numeric(dataset$Signal/dataset$BG) # add signal to noise ratio

# convert timestamp & sort ascendic for timestamp
dataset$ts <- as.POSIXct(as.numeric(as.character(dataset$TS_num)),origin="1970-01-
      01",tz="GMT") # GMT! to obtain local time; double check for your own data
dataset$Year <- as.numeric(format(dataset$ts,format="%Y"))
dataset <- dataset[order(dataset$TS_num),]   # sort rows by timestamp
rownames(dataset) <- NULL                     # ascending row numbers

# save data frame so that it can be loaded easily for the next steps**
# write.csv(dataset,paste(directory,"dataset_WinterTelemetry.csv",sep="/"), row.names
      = FALSE)
```

* The SG records any information and receives signals in a *txt* file that is compressed to *txt.gz* after one hour. The previous *txt* file is deleted. Two new files are created for the data collection of the next hour: a *txt* and an empty *txt.gz* file. In case of interruptions or during the data download, the data might not be compressed into the *txt.gz* file yet. Then, the available data can be extracted from the *txt* file directly.

** To avoid re-running the script and subsequently waiting for the processing time multiple times, we saved the data frames of the intermediate steps as *csv* files that can be easily read in before progressing with the pipeline. Note that the file size can be very large depending on the amount of data (e.g. 1.2 GB for ca 8.5 x 10^6 rows in the raw data).

Table S2_2.1: Raw data output from the SensorGnome in columns 1-6. The Info column indicates if the row contains a record about a change in settings (S) or a received radio signal (pX, which contains the port number X and is equal to the antenna number, e.g. p4). Depending on the row type, the following columns contain different information which can be extracted and separated, accordingly: TS_num contains the numeric timestamp in seconds from epoch 1970-01-01, and V2 the antenna (= Antenna) of which settings are changed or the deviation of signal from the set frequency (= dfreq, kHz). V3 has information about which setting is changed (= Setting) or the relative signal strength (= Signal, -100 to 0 dB), and V5 about the value of the new setting (= Setting_Value) or the relative level of background noise (= BG, -100 to 0 dB).

Info	TS_num	V3	V4	V5	V6	Site	Receiver	Antenna	dfreq	Setting	Signal	Setting_Value	BG	SNR
S	1644098402.255	8.000	frequency	150.640		GRO	LB	p8	NA	frequency	NA	150.64	NA	NA
S	1644098402.207	5.000	frequency	150.640		GRO	LB	p5	NA	frequency	NA	150.64	NA	NA
S	1644098402.230	6.000	frequency	150.640		GRO	LB	p6	NA	frequency	NA	150.64	NA	NA
S	1644098402.278	7.000	frequency	150.640		GRO	LB	p7	NA	frequency	NA	150.64	NA	NA
p4	1644098402.405	4.631	-68.13	-74.98	NA	GRO	LB	p4	4.631	NA	-68.13	NA	-74.98	0.909
p4	1644098402.408	4.791	-70.2	-75.64	NA	GRO	LB	p4	4.791	NA	-70.20	NA	-75.64	0.928
S	1644098402.184	4.000	frequency	150.640		GRO	LB	p4	NA	frequency	NA	150.64	NA	NA
p8	1644098403.416	3.867	-68.71	-77.92	NA	GRO	LB	p8	3.867	NA	-68.71	NA	-77.92	0.882
p8	1644098403.418	4.019	-74.26	-79.06	NA	GRO	LB	p8	4.019	NA	-74.26	NA	-79.06	0.939
p8	1644098404.791	4.207	-68.66	-78.02	NA	GRO	LB	p8	4.207	NA	-68.66	NA	-78.02	0.880

Set frequencies and other settings were assigned to the radio signals passing chronologically through the rows so that the radio signals can be matched to the transmitter monitored. Additionally, we flagged detections within the first second after a

frequency change for a later filtering step because those turned out to be problematic due to a carry-over of signals from the previous frequency (see Section 3.1).

```
#### 2.3. Assigning Frequencies ####
# split into antennas
dataset2 <- split(dataset, f=list(dataset$Year,dataset$Site,dataset$Receiver,
      dataset$Antenna,drop=T),drop=TRUE)

# assign set frequencies
for(a in seq_along(dataset2)){

  dataset2[[a]] <- dataset2[[a]][order(dataset2[[a]]$TS_num),] # sort rows by
                                                                 timestamp
  rownames(dataset2[[a]]) <- NULL           # rename rows in the ascending order

  # vectorisation to speed up loop
  # initialisation of results: create NA vectors
  Freq <- as.numeric(rep(NA,nrow(dataset2[[a]])))
  ChangeFilter <- as.numeric(rep(NA,nrow(dataset2[[a]])))
  SecondFilter <- as.numeric(rep(NA,nrow(dataset2[[a]])))

  # conditioning: create TRUE/FALSE vectors for required if statements
      # setting row for switching frequency
  SetFreq <- c(grepl("S", dataset2[[a]]$Info) & dataset2[[a]]$Setting == "frequency")
  Detection <- c(grepl("p", dataset2[[a]]$Info)) # detection row
  TimeInBetween <- c(NA,diff(dataset2[[a]]$TS_num)) # time interval between rows

  # initial variables needed to start the loop
      # first frequency set
  current_freq <- dataset2[[a]]$Setting_Value[which(SetFreq==TRUE)][1]
      # first time of frequency setting
  change_time <- dataset2[[a]]$TS_num[which(SetFreq==TRUE)][1]

  # processing all rows in data row-by-row
  for(i in 1:length(dataset2[[a]]$Info)){
    # is it a setting row with frequency changes (TRUE/FALSE)
    if(SetFreq[i]){
      current_freq <- dataset2[[a]]$Setting_Value[i] # extract the new frequency
      Freq[i] <- current_freq                      # assign this frequency to the row

      change_time <- dataset2[[a]]$TS_num[i]   # extract the time of frequency change
    }
    # is it a row with detection (radio signals)
    if(Detection[i]){
      Freq[i] <- current_freq # assign current frequency

      # mark detections that occur within 1st sec after change (check millisec)
      ChangeFilter[i] <- ifelse(dataset2[[a]]$TS_num[i]-change_time < 1,TRUE,FALSE)
      # TRUE/1 for filter, FALSE/0 for keep
      }
  }
  dataset2[[a]]$Freq <- Freq                # add the frequency vector to the dataset
  dataset2[[a]]$ChangeFilter <- ChangeFilter         # add the change filter
}
```

```r
# merge the list of datasets and remove the created row names so that they are just
# numbered
dataset_conv <- do.call("rbind",dataset2)
rownames(dataset_conv) <- NULL

# write.csv(dataset_conv,paste(directory,"dataset2_WinterTelemetry.csv",sep="/"),
      row.names = FALSE)
```

Then, we selected signals only and assigned the individual IDs. For this, we merged the records with a data frame that contained the BirdID, year, site and the frequency of the transmitter used. Please, note that it is recommended to set the frequencies 4 kHz lower at the SG receiver (see above) so that this needs to be taken into account in the data frame with the individual information.

Table S2_2.2: Radio signals (detections), their qualitative properties, assigned frequency, individual ID and other information: Both, TS_num and ts, represent the timestamp in numeric form (in seconds from epoch 1970-01-01) and date-time format, respectively. dfreq shows the deviation between recorded and set frequency in kHz. Signal and BG are the relative strength (in dB; log scale with 0 at maximal strength) of the signal and the background noise (BG), respectively. From those, the signal-to-noise ratio (SNR) was calculated. Freq contains the set frequency, and detections that are within one second after the switch of the frequency are marked in ChangeFilter. The last columns give information about the individual ID (BirdID), location (Site) and the receiver (Receiver, Antenna).

TS_num	ts	dfreq	Signal	BG	SNR	Freq	ChangeFilter	BirdID	Site	Receiver	Antenna
1644098402.405	2022-02-05 23:00:02	4.631	-68.13	-74.98	0.909	150.640	remove	BD58563	GRO	LB	p4
1644098402.408	2022-02-05 23:00:02	4.791	-70.20	-75.64	0.928	150.640	remove	BD58563	GRO	LB	p4
1644098422.890	2022-02-05 23:00:22	4.157	-67.57	-75.32	0.897	150.779	remove	BD58566	GRO	LB	p4
1644098422.892	2022-02-05 23:00:22	4.165	-62.17	-74.41	0.836	150.779	remove	BD58566	GRO	LB	p4
1644098424.600	2022-02-05 23:00:24	3.879	-62.11	-74.49	0.834	150.779	keep	BD58566	GRO	LB	p4
1644098426.314	2022-02-05 23:00:26	3.871	-62.42	-74.61	0.837	150.779	keep	BD58566	GRO	LB	p4
1644098426.321	2022-02-05 23:00:26	4.295	-67.51	-75.25	0.897	150.779	keep	BD58566	GRO	LB	p4
1644098428.026	2022-02-05 23:00:28	4.050	-67.59	-75.42	0.896	150.779	keep	BD58566	GRO	LB	p4
1644098428.026	2022-02-05 23:00:28	3.910	-62.28	-74.81	0.833	150.779	keep	BD58566	GRO	LB	p4
1644098429.747	2022-02-05 23:00:29	4.285	-67.60	-75.11	0.900	150.779	keep	BD58566	GRO	LB	p4

* For further information see the archived SensorGnome documentation, e.g. at *The Web Interface* tab (https://archived.sensorgnome.org/).

3. Filtering

Now, we filtered the data addressing several issues associated with the raw SG data: First, we found a carry-over effect of radio signals from one to the next frequency sampled, probably caused by a time lag between hard- and software (Section 3.1). Second, telemetry antennas can detect the radio signal, and its echo, from multiple angles resulting in artefacts such as multiple detections of the same signal per second (Section 3.2 – 3.3). Additionally, the SG software might further fragment the signal (Section 3.3). All this results in noise that obscure the actual radio signal and is visible in the raw data file:

Table S2_3: This extract from the raw data shows a switch of the set frequency in antenna 'p5' (row 1, green) followed by multiple detections thereafter. The timestamps, ts and TS_num, enable us to spot multiple detections per second easily. The ChangeFilter column already marks which detections are within a second after a frequency switch (= 'remove'). However, there are still more detections than emitted radio signals thereafter, e.g. multiple detection per second (indicated by colour).

Info	ts	TS_num	Freq	dfreq	Signal	BG	SNR	ChangeFilter
S	2022-02-08 23:00:42	1644357642.211	150.256	NA	NA	NA	NA	NA
p5	2022-02-08 23:00:42	1644357642.314	150.256	4.998	-66.28	-73.63	0.900	remove
p5	2022-02-08 23:00:42	1644357642.315	150.256	5.004	-65.58	-73.30	0.895	remove
p5	2022-02-08 23:00:44	1644357644.079	150.256	4.639	-66.79	-73.92	0.904	keep
p5	2022-02-08 23:00:44	1644357644.079	150.256	4.643	-66.01	-73.65	0.896	keep
p5	2022-02-08 23:00:45	1644357645.857	150.256	4.989	-66.58	-73.64	0.904	keep
p5	2022-02-08 23:00:45	1644357645.859	150.256	4.998	-65.64	-73.26	0.896	keep
p5	2022-02-08 23:00:47	1644357647.626	150.256	4.715	-65.83	-73.34	0.898	keep
p5	2022-02-08 23:00:47	1644357647.629	150.256	4.960	-66.55	-73.69	0.903	keep
p5	2022-02-08 23:00:49	1644357649.399	150.256	4.713	-66.32	-72.86	0.910	keep
p5	2022-02-08 23:00:49	1644357649.400	150.256	4.910	-65.37	-72.67	0.900	keep

3.1. Carry-over from previous frequency

In the raw data we found subsequentially recorded frequencies showing the same, overlapping pattern in *dfreq* which infers that the subsequential frequency contained some detections aligning with previously sampled frequency (Figure S2_3.1 a). These detections are closely associated to the change of the frequency in the receiver (Figure S2_3.1 b). This carry-over effect is probably caused by the software (i.e. Raspberry Pi) changing before and/or quicker than the hardware (i.e. antenna).

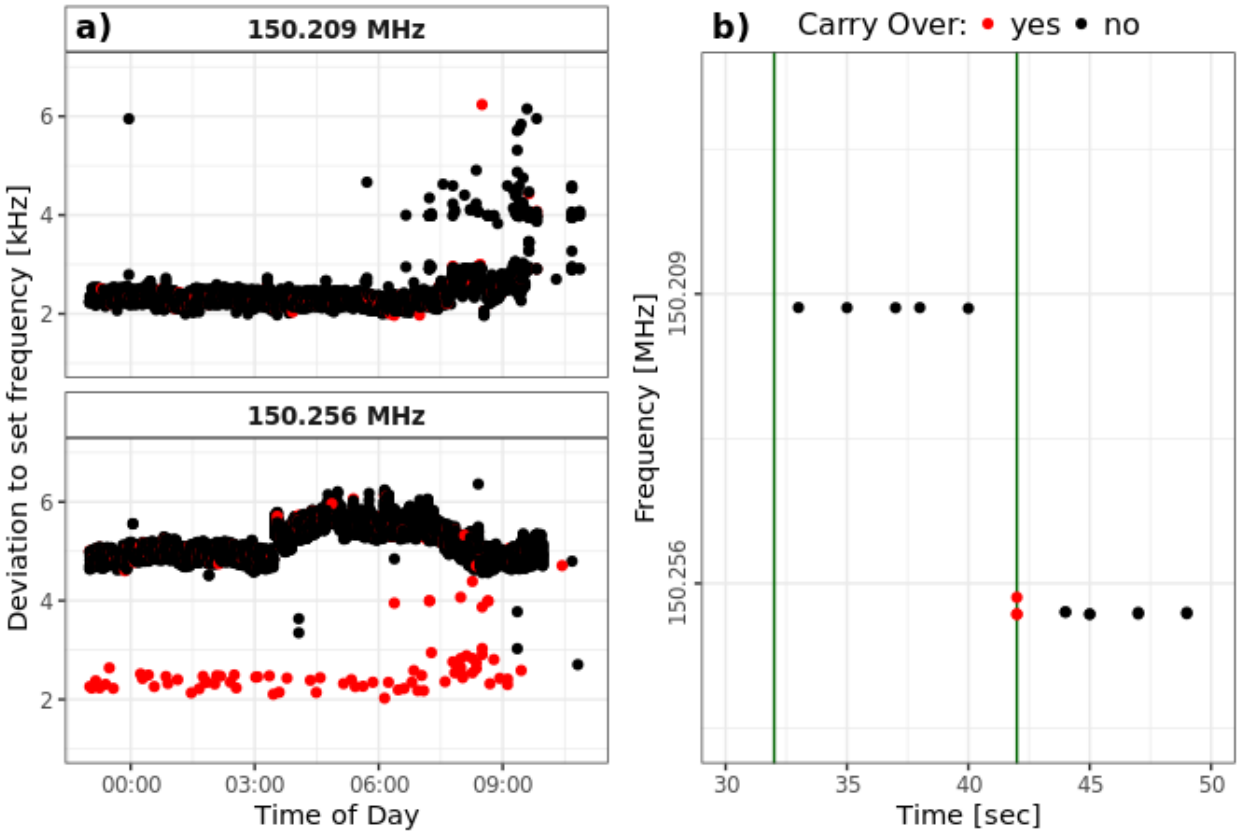

Figure S2_3.1: The carry-over effect: a) Two subsequent example frequencies show the same pattern of deviations. Detections within one second after the transition from the previous frequency are marked red. b) Detail of a frequency change (vertical green lines) in the software.

Solution: Removal of detections that are within 1 sec after a frequency change

```
#### 3.1. Filter: remove detections within one second after frequency change ####
# subset to detections more than 1 sec after frequency switch
dataset_filt1 <- subset(tags, ChangeFilter==0)
```

3.2. Background noise & tag signal artefacts

Strong noise can obscure the signal and not every detection is a true signal. In the SG software (i.e. in deployment.txt file) it is recommended by the developers that the frequency is set 4 kHz below the carrying frequency of a tag (the frequency provided by a supplier) so that we expect *dfreq* to be around 4 kHz. As a first step, we visually inspected the histograms for *dfreq* and background noise (*BG*) per transmitter. In our study, most detections fell into a range of 2 – 7 kHz for *dfreq* and -70 to -86 dB for *BG*. Thus, we selected detections with more than 1.5 kHz *dfreq* and *BG* below -70 dB. Note that these thresholds can vary depending on the used SG settings, the transmitters, and the circumstances of the area regarding background noise levels so that they need to be chosen based on the collected data. Additionally, the recorded frequency can vary with environmental cues such

as ambient temperature, and often also shows artefacts (multiples of the main carrying frequency of a tag). Thus, we split the data into nights (24-h bins) and further into distributions (similar to Figure S2_3.3 b). We assigned distribution numbers to every data point within each night, before picking the detection from the largest distribution per minute. To further smooth the data, we applied a *hampel* filter to remove outliers (Jonasson 2017). The *hample* filter removes outliers that deviate from the median in a time series using a sliding window (with length set in *k*) and a given threshold (set in *t0*).

Solution: Removal of detections with strong background noise and wrong frequencies

```
# split the data to process with the filtering separately for every transmitters-
antenna combination
dat_antenna <- split(dataset_filt1, f = list(dataset_filt1$Year,dataset_filt1$BirdID,
       dataset_filt1$Receiver,dataset_filt1$Antenna), drop=TRUE)
# the following code can be applied to every transmitter-antenna combination using
  for loop going through the list of data frames

#### 3.2. Filter: remove very high BG noise & artefacts in dfreq ####
# general filter: completely wrong BG and dfreq
# values are chosen by visual inspection of all data, i.e. distribution of data
  points for every frequency. We selected dfreq larger than 1.5 kHz and BG noise
  weaker than -70 dB
dat_antenna2 <- subset(dat_antenna, dfreq>1.5 & BG< (-70))

# dfreq: filter multiple dfreq detected per signal
# after each data point is assigned distributions of dfreq per 24 h (just like for BG
  later, see Figure S2_3.3b), the detections from the largest distribution are chosen
  per minute
data_antenna2 <- dat_antenna2 %>%
  # create two types of bins: AnalysisDate (i.e. 24 h shifted by -12 h so this is
equivalent to night) and 1-min bins
  mutate(AnalysisDate = as.factor(format(ts+12*60*60,format="%Y-%m-%d")),
         bin = floor(TS_num/60)) %>%
  ungroup() %>% group_by(AnalysisDate) %>% # per 24 h (here, split by 12:00)
  # check for multimodality (multi) and assign distribution numbers and parameters
  mutate(multi = dip.test(dfreq)$p.value<0.05,
         distr.nr = ifelse(multi,densityMclust(dfreq, # total number of distributions
                    modelNames="E",plot=FALSE)$G,1),
         distr = ifelse(multi,densityMclust(dfreq,              # distribution number
                  modelNames="E",plot=FALSE)$classification, 1),
         distr.size = ifelse(multi,densityMclust(dfreq,    # size of the distribution
                  modelNames="E",plot=FALSE)$parameters$pro[distr],1)) %>%
  group_by(bin) %>% # per 1-min bin
  # choose the detections from the larger distribution (==0)
  mutate(dfreqFilter = ifelse(distr.size!=max(distr.size),1,0))

filtered <- data_antenna2 %>% filter(dfreqFilter==0) %>%     # apply filter
  dplyr::select(-c(contains("distr"),multi)) %>% ungroup()   # remove "multi"-columns

# dfreq: hampel filter
outliers <- hampel(filtered$dfreq, k=100,t0=1.5) # find outliers
filtered <- filtered[-c(outliers$ind),]          # remove outliers
```

3.3. Artefacts in BG & multiple detections per second

The raw data can show multiple detections of the same signal. These detections differ in signal strength, SNR, and BG noise. Signal strength and therefore also SNR varies depending on the activity of the individual and can therefore not be used to filter the data. However, BG noise strength is supposed to be stable overtime with no sudden changes. Similar to the previous 'distribution' filter, we split the data, assigned distribution numbers to the data points (Figure S2_3.3 b), and picked the detections from the largest distribution, before smoothing the time series with a *hampel* filter. In case there were still multiple detections per second left over, we picked the first.

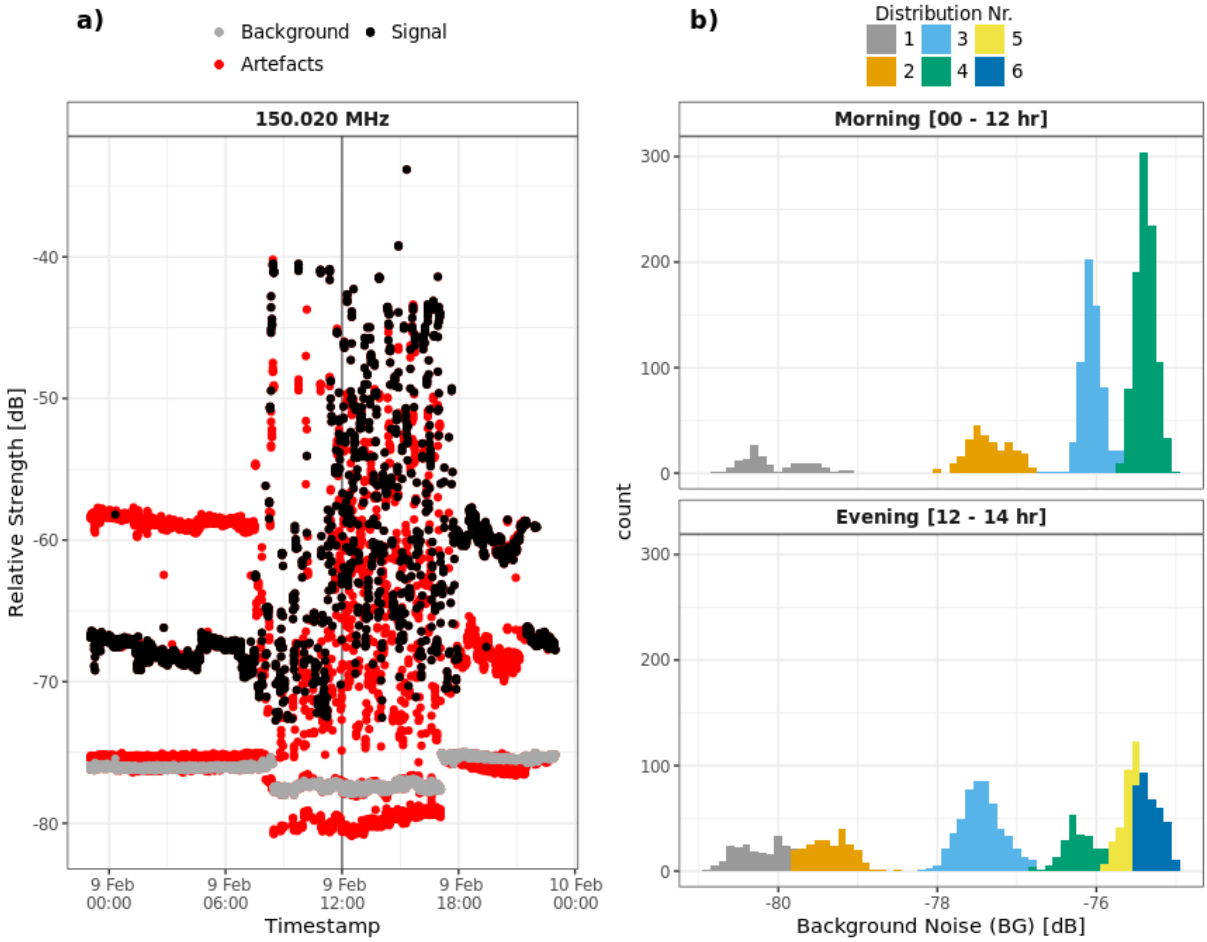

Figure S2_3: The Background noise (BG) artefacts: a) Time series dfreq and BG showing multiple timeseries each. Filtered data in red. b) Histogram BG noise for first and second part of a given date. Notice that values of background noise tend to cluster forming multimodal patterns.

Solution: Inclusion of detection from one stable BG noise and, if necessary, the first one per second

```
#### 3.3. Filter: remove BG artefacts & multiple detections per second ####
# BG noise: filter multiple BG detections per signal
# after each data point is assigned distributions of dfreq per 24 h (see Figure
  S2_3.3b), the detections from the largest distribution are chosen per minute
filtered <- filtered %>%
  ungroup() %>% group_by(AnalysisDate) %>% # per 24 h (here, split by 12:00)
  # check for multimodality (multi) and assign distribution numbers and parameters
  mutate(multi = dip.test(BG)$p.value<0.05,
         distr.nr = ifelse(multi,densityMclust(BG,                    # total number
                    modelNames="E",plot=FALSE)$G,1),
         distr = ifelse(multi,densityMclust(BG,                # distribution number
                 modelNames="E",plot=FALSE)$classification,1),
         distr.size = ifelse(multi,densityMclust(BG,                  # size
                      modelNames="E",plot=FALSE)$parameters$pro[distr],1)) %>%
  group_by(bin) %>% # per 1-min bin
  # choose the detections from the larger distribution (==0)
  mutate(BGFilter = ifelse(distr.size!=max(distr.size),1,0))

filtered2 <- filtered %>% filter(BGFilter==0) %>% # apply filter
  dplyr::select(-c(contains("distr"),multi)) %>% ungroup()

# BG noise: hampel function
outliers2 <- hampel(filtered2$BG, k=100,t0=1.5) # find outliers
filtered3 <- filtered2[-c(outliers2$ind),]      # remove outliers

# filter one per sec:
# in case there are still multiple data points per second, the first one is chosen
filtered3$TS_num <- as.numeric(filtered3$TS_num)
TimeInBetween <- c(NA,diff(filtered3$TS_num))   # conditioning
prevDetect_time <- filtered3$TS_num[1]-1        # 1 sec before first detection
SecondFilter <- as.numeric(rep(NA,nrow(filtered3)))
for(a in 1:nrow(filtered3)){
  # choose 1st detection (multiple detections within sec, from echo or SG)
  SecondFilter[a] <- ifelse(filtered3$TS_num[a]-prevDetect_time <1,  TRUE, FALSE)
      # TRUE for remove, FALSE for keep
  prevDetect_time <- ifelse(SecondFilter[a]==FALSE,filtered3$TS_num[a],
              prevDetect_time) # time of (real) detection if its not filtered against
}

filtered3$SecondFilter <- SecondFilter
filtered4 <- subset(filtered3, SecondFilter==0)  # apply filter
```

4. Activity & Skin Temperature

From the filtered data, we extracted changes in signal strength as a measure of activity and assigned recorded temperatures to the signals. Similar to the filtering, this was done separately for every frequency and antenna used, which were merged together afterwards.

4.1. Activity

Signal strength varies with distance and movement of the transmitter. Therefore, its variation is equivalent to the relative activity of the tagged individual. Low variation is expected for low movement i.e. activity levels, and high variation for high activity levels, respectively. Therefore, we first averaged the data into 5-min bins and then calculated the deviation in signal strength between subsequent bins.

4.2. Skin Temperature

To assign skin temperature values, we followed the pipeline from Jonasson (2017). We calculated the interval between two signals using the numeric timestamp (including milliseconds), filtered for appropriate intervals and applied the tag-specific calibration curves (Figure S2_4.1). Tag-specific curves were obtained from the calibration of the tags using a progressively cooling water bath.

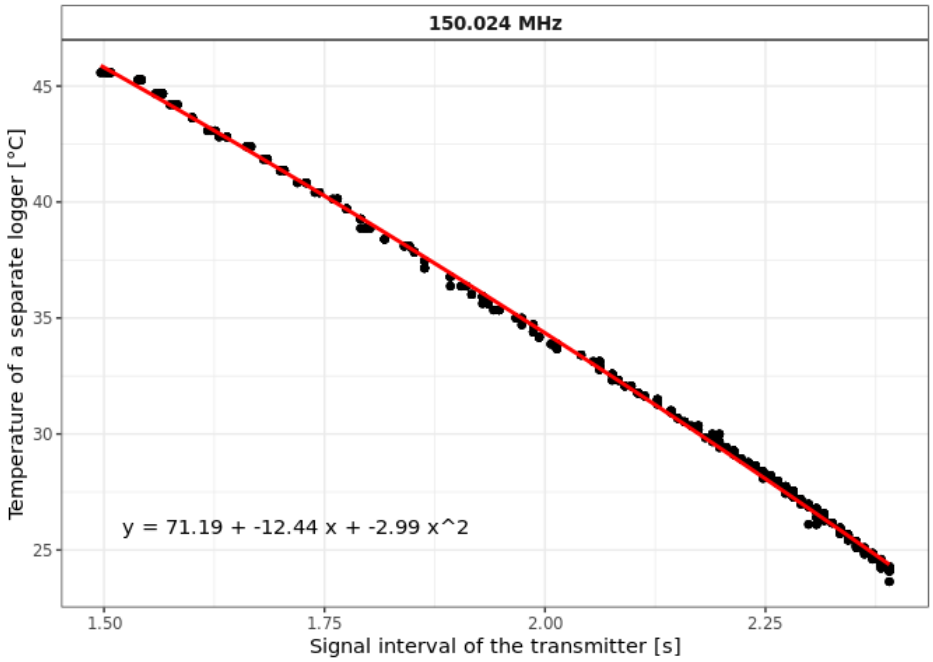

Figure S2_4.1: An example of a calibration curve.

```
#### 4. Activity & Skin Temperature ####
# split the data to process with the filtering separately for every individual and
  year
dataset3 <- split(Filtered_data,
                  f = list(as.factor(Filtered_data$BirdID),
                           as.factor(Filtered_data$Freq)), drop=TRUE)
```

```r
# lists for output data
Activity_all <- list()
Skin_Temp_bird <- list()

# data analysis per year-individual combination
for(i in 1:length(dataset3)){
  # extract data and information
  dat_freq <- dataset3[[i]]
  freq <- unique(dat_freq$Freq)
  bird <- unique(dat_freq$BirdID)
  year <- unique(dat_freq$Year)

  # data analysis per antenna: split data and go through the list of data frames
  dat_antenna <- split(dat_freq,dat_freq$Antenna,drop=TRUE)
  for(b in 1:length(dat_antenna)){
    antenna <- unique(dat_antenna[[b]]$Antenna) # extract antenna info

#### 4.1. Activity ####
    # data binning
    binsize <- 5 # in min
    dat_antenna[[b]]$datetime_num <- floor(dat_antenna[[b]]$TS_num/60/binsize)*
                                     binsize # datetime in 5-min bins
    # averaging of recorded skin temperature and signal strength (for activity) for
      each bin and individual
    Activity <- aggregate(Signal ~ datetime_num+BirdID+Freq+Receiver+Antenna,
                          data=dat_antenna[[b]],FUN=mean) %>%
      rename(Pwr = "Signal") %>%
      mutate(ts = as.POSIXct(datetime_num*60,origin="1970-01-01",tz="CET"))
         # needs to be CET to be actually CET

    # fill missing values with NA
    # select bird specific time period
    Time_min <- min(Activity$ts)
    Time_max <- max(Activity$ts)
    # create data frame with all bins possible
    full_time <- data.frame(ts=as.POSIXlt(c(seq(Time_min,Time_max,by=binsize*60)),
                                tz="CET")) # needs to be CET to be actually CET
    # merge with existing data frame
    Activity <- merge(full_time,Activity,by=c("ts"),all=TRUE)
    Activity <- Activity[order(Activity$ts),] #order by date and time
    rownames(Activity) <- NULL
    Activity$Timestamp_num <- as.numeric(as.POSIXct(Activity$ts)) # add missing cells

    # add deviation of signal strength as measure for activity
    Activity$Pwr_diff <- abs(c(NA, diff(Activity$Pwr)))

    Activity_bird[[b]] <- Activity

#### 4.2. Skin Temperature ####
    # prepare new columns
    dat_antenna[[b]]$beep_int <- NA      # interval between signals
    dat_antenna[[b]]$rel_beep_int <- NA  # realistic interval? (filter)
    dat_antenna[[b]]$skin_temp <- NA     # calculated skin temperature
```

```
    dat_antenna[[b]]$rel_skin_temp <- NA # realistic skin temperature? (filter)
    # check for enough data to skip antennas with little information
    if(nrow(dat_antenna[[b]])<200){
      print(paste("skipped: i is",i,"- data from bird",bird, freq, antenna, "have
                  only", nrow(dat_antenna[[b]]),"(<200) data records",sep=" "))
      }else{
      # sort by timestamp
      dat_antenna[[b]]$TS_num <- as.numeric(dat_antenna[[b]]$TS_num)
      dat_antenna[[b]] <- dat_antenna[[b]][order(dat_antenna[[b]]$TS_num),]

      # calculate time intervals
      dat_antenna[[b]]$beep_int <- c(NA,diff(dat_antenna[[b]]$TS_num))

      # remove improbable time intervals
      # minimum 20bpm (usually min is 25bpm) -> 3 sec interval max
      # maximum 50bpm (usually max is 45bpm) -> 1.2 sec interval min
      dat_antenna[[b]]$rel_beep_int <- as.factor(ifelse(dat_antenna[[b]]$beep_int>
                                       1.2 & dat_antenna[[b]]$beep_int< 3,TRUE,FALSE))
          # TRUE/1 for keep, FALSE/0 for filter


      # apply skin temperature function: y ~ intercept + slope1*x + slope2*x^2
      cal_row <-  which(calibration$Year==year & calibration$Freq_SG == freq)
      dat_antenna[[b]]$skin_temp <- calibration$Intercept[cal_row] +
                           (calibration$Slope1[cal_row]*dat_antenna[[b]]$beep_int) +
                           (calibration$Slope2[cal_row]*dat_antenna[[b]]$beep_int^2)

      # mark improbable skin temperatures: lower than 20 °C, larger than 50 °C
      dat_antenna[[b]]$rel_skin_temp <- as.factor(ifelse(dat_antenna[[b]]$skin_temp>
                                      20 & dat_antenna[[b]]$skin_temp< 50,TRUE,FALSE))
          # TRUE/1 for keep, FALSE/0 for filter
    }
  }
  # save activity into list if there is any available, and save skin temperature
  if(length(Activity_bird)>0){
    Activity_all[[i]] <- do.call("rbind",Activity_bird) # save activity
  }
  Skin_Temp_bird[[i]] <- do.call("rbind",dat_antenna) # save temperature
}

# merge the lists of datasets
Activity_data <- do.call("rbind",Activity_all)
Skin_Temp_all <- do.call("rbind",Skin_Temp_bird)

# write.csv(Activity_data,"dataset_Winter_activity_20231018.csv", row.names = FALSE)
# write.csv(Skin_Temp_all,"Skin_Temp_Winter_20231018.csv", row.names = FALSE)
```

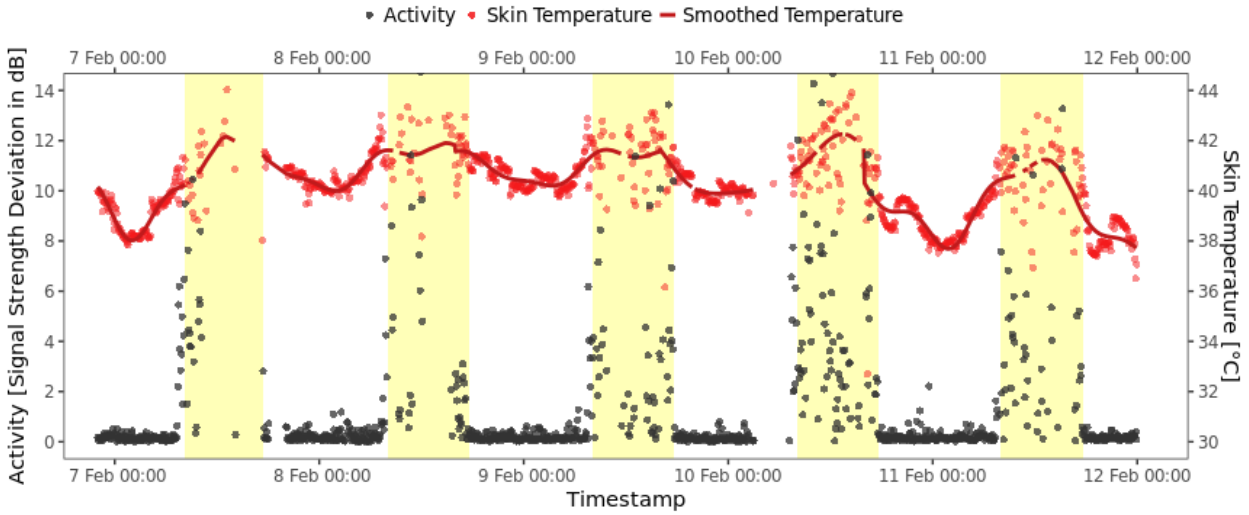

Figure S2_4.2: An example of activity (black dots) and skin temperature patterns (light red dots for filtered, and dark red line for smoothed data) across time. Yellow shades indicate daylight periods.

5. Functions for Onset & Offset

Following Strauß et al.'s (2022) pipeline for extraction of onset and offset for activity and skin temperature, we used the filtered and converted data to choose analyses windows and to extract chronotype traits thereafter.

For activity onset and offset we adjusted a behavioural change point analysis (BCPA, from Dominoni et al. 2014 and Strauß et al. 2022). In the BCPA, two distributions were fitted to the data of the chosen analysis window separating active and inactive phase. This was done for all possible changepoints, of which the most plausible was chosen, i.e. with the lowest Akaike information criterion (AIC). A reliable BCPA requires sufficient data i.e. less than 30% data gaps within the analysis window. The required data were not always available in our study because some individuals left the detection area of the receiver in their active phase creating data gaps during daytime. Therefore, we also used a threshold of 4 dB (adjusted from Adelman et al. 2010) to extract onset and offset of activity when sufficient data were available during night-time.

```
#### 5.1. Onset & Offset of Activity ####
# variables required for change point functions
per_h <- 24            # set length of expected period in hours: here 24 h
per_sec <- per_h*60*60 # period in sec
binsize <- 5           # bin size in min
window_size <- 8       # for activity function
bins_possible <- window_size*60/binsize
window_length <- 5     # for BCPA

# BCPA function to assign AICs for every possible change points
bcpa_actday_function <- function(x){
  library(MASS)
```

```
  # length of window (10 data points)
  window_length <- window_length
  # normal distribution
  dist<-"normal"
  # x is a data frame
  x <- as.data.frame(subset(x,(!is.na(x$Pwr_diff))))
  # consider empty data frames
  if (nrow(x)>0){
    # there need to be more than 70% of data points
    if(nrow(x)<bins_possible*0.70){
      # assign NA to AIC column
      x[,"AIC"] <- NA
    }else{
      # from 5 data points in, to 5 data points from end
      for( d in window_length:(nrow(x)-window_length)){
        # calculate AIC by summing logliks of the 2 distributions
        x[d,"AIC"]<-AIC(

          # two normal distributions are fitted to the data,
          # one for the data before a given time point and one for the data after
          # given time point and calculates log likelihood
          logLik(fitdistr((x[,'Pwr_diff'])[1:d],'normal'))+
            logLik(fitdistr((x[,'Pwr_diff'])[(d+1):nrow(x)],'normal')))
        x$AIC <- ifelse(is.infinite(x$AIC),NA,x$AIC) #removes infinites
      }
    }
    # keep intervals and AIC column
    AICs <- x[, c('Year', 'Site','BirdID', 'window','JulianDay', 'Hours_num', 'AIC')]
  }
  return(AICs)
}

# Onset & Offset from BCPA
onoff_act_function <- function(x){
  bcpa_act <- NA
  #has AIC values (not just NA)
  if(nrow(x[!is.na(x$AIC),])>0){
    x <- as.data.frame(x)
    #selection of lowest AIC
    min_AIC <- aggregate(AIC~ Year+Site+BirdID+window+JulianDay,x, FUN="min",na.rm=T)
    bcpa_act <- merge(min_AIC,x,by=c("Year","Site","BirdID","JulianDay","window",
                                     "AIC"),all.x=TRUE,all.y=FALSE)
  }
  return(bcpa_act)
}

# 4dB-threshold method
temp_thres <- 4 # threshold in dB
binsize <- 5    # bin size in min
db_day_function <- function(x){
  BirdID <- NA
  Year <- NA
  JulianDay <- NA
  AMPM <- NA
```

```
  db.Chrono <- NA
  # extract information
  BirdID <- unique(x$BirdID)
  Year <- unique(x$Year)
  JulianDay <- unique(x$JulianDay)
  AMPM <- unique(x$AMPM)
  Site <- unique(x$Site)
  # get GPS coordinates and calculate sunrise and sunset
  gps <- subset(GPS,Site==unique(x$Site))
  Date <- format(as.POSIXct(paste(unique(x$Year),unique(x$JulianDay)),format="%Y %j"),
                 format="%Y-%m-%d")
  sunrise_num <- as.numeric(times(format(as.POSIXct(getSunlightTimes(date=
                              as.Date(Date),lat=gps$Lat,lon=gps$Lon,tz="CET")$sunrise),
                     format="%H:%M:%S")))*24 # set differently for different locations
  sunset_num <- as.numeric(times(format(as.POSIXct(getSunlightTimes(date=
                               as.Date(Date),lat=gps$Lat,lon=gps$Lon,tz="CET")$sunset),
                     format="%H:%M:%S")))*24

  # number of possible bins: night-time after or before midnight for onset or offset,
    respectively
  bins_possible <- ifelse(AMPM=="AM",sunrise_num*60/5,(24-sunset_num)*60/5)
  # available bins
  bins_available <- ifelse(AMPM=="AM",nrow(x[x$Hours_num<sunrise_num,]),
                                      nrow(x[x$Hours_num>sunset_num,]))

  # there need to be more than 70% of data points available at night-time before or
    after midnight
  if(bins_available>0.7*bins_possible){
    if(AMPM=="AM"){
      # select non-active part i.e. <4dB
      sub <- x %>% filter(window=="AM") %>%
        mutate(time = min(Hours_num[Pwr_diff>temp_thres],na.rm=T)) %>%
        filter(Hours_num<time)
      # one bin after inactivity
      db.Chrono <- max(sub$Hours_num[which(sub$Pwr_diff<temp_thres)],na.rm=T)+
                   binsize/60
    }else{
      # select non-active part i.e. <4dB
      sub <- x %>% filter(window=="PM") %>%
        mutate(time = max(Hours_num[Pwr_diff>temp_thres],na.rm=T)) %>%
        filter(Hours_num>time)
      # one bin before inactivity
      db.Chrono <- min(sub$Hours_num[which(sub$Pwr_diff<temp_thres)],na.rm=T)-
                   binsize/60
    }
  }

  db.Chrono <- ifelse(db.Chrono==Inf | db.Chrono==-Inf,NA ,db.Chrono)
  db.method <- data.frame(Year,Site,BirdID,AMPM,JulianDay,db.Chrono)

  return(db.method)
}
```

All onsets and offsets were visually inspected, and unreliable ones were marked for removal. The results from both methods were highly correlated so that, for statistical

analysis, we used BCPA onsets and offsets filled up with the ones from the 4dB-threshold method (where available, Figure S2_5).

Similarly, we extracted skin temperature onsets using the first rise in morning (adjusted from Strauß et al. 2022). To do so, we first smoothed the data using a sinusoidal curve with three harmonics, and then extracted the first rise (> 0 change) of skin temperature before re-warming in the morning. The output was also visually inspected (Figure S2_5).

```
#### 5.2. Minimum Skin Temperature ####
cptday_function <- function(x){
  BirdID <- NA
  AnalysisDate <- NA
  AMPM <- NA
  cpt.change <- NA
  cpt.min <- NA
  cpt.max <- NA
  diff.min <- NA
  diff.change <- NA
  diff.max <- NA

  # bins possible before sunrise
  bins_possible2 <- bins_possible -
                    (ifelse(unique(x$AMPM)=="AM",10-unique(x$Sunrise_num),0))*60/5

  # differences (slope) between temperatures
  x$Temp_diff <- c(NA, diff(x$Est_Temp))            # add deviation from previous bin
  x$Temp_diff <- ifelse(abs(x$Temp_diff)>1,NA,x$Temp_diff)
     # remove outliers from data gaps

  x <- as.data.frame(subset(x,is.na(Est_Temp)!=TRUE))
  bins_available <- c(nrow(subset(x,AnalysisHour<Sunrise_num)),
                    nrow(subset(x,AnalysisHour<Sunrise_num & is.na(x$Skin_Temp)==F)))

  # consider empty data frames
  if(nrow(x)>0){
    BirdID <- unique(x$BirdID)
    AnalysisDate <- unique(x$AnalysisDate)
    AMPM <- unique(x$AMPM)
    # consider only windows with 80% of data and maximal 10% of this interpolated
    if(bins_available[1]<bins_possible2*0.8 & bins_available[2]<bins_possible2*0.7){
      cpt.change <- NA
      cpt.min <- NA
      cpt.max <- NA
      diff.min <- NA
      diff.change <- NA
      diff.max <- NA
    }else{
      # for onset only
      increase <- x %>%
        # narrow window to time of period that contains increasing temperatures
        filter(AnalysisHour>= min(AnalysisHour[which(Temp_diff>=0)])
               & AnalysisHour<= max(AnalysisHour[which(Temp_diff>=0)])) %>%
```

```
        # extract positive changes in temperature of >= zero → increases
        filter(Temp_diff>=0 &
        # and, in case of negative changes i.e. decreasing temperature, only select
          hours that are after the steepest decrease → this filters some cases where
          skin temperature spontaneously warms up at night-time

              AnalysisHour >= ifelse(min(Temp_diff,na.rm=TRUE)<0 &
                          AnalysisHour[which(Temp_diff==min(Temp_diff,na.rm=TRUE))]<
                             mean(AnalysisHour,na.rm=TRUE),
                          AnalysisHour[which(Temp_diff==min(Temp_diff,na.rm=TRUE))],
                          min(AnalysisHour)))
      if(nrow(increase)>1){
        # absolute change (here always increase)
        increase$Temp_diff <- abs(increase$Temp_diff)
        # minimum skin temperature
        increase_early <- subset(increase,AnalysisHour==min(increase$AnalysisHour))
        cpt.min <- increase_early$AnalysisHour # time at min temperature
        diff.min <- increase_early$Temp_diff   # change at min temperature
        }
    }
  }

  cpt_output <- data.frame(BirdID, AnalysisDate, cpt.min,cpt.change,cpt.max,
diff.min,diff.change,diff.max,AMPM)
  return(cpt_output)
}
```

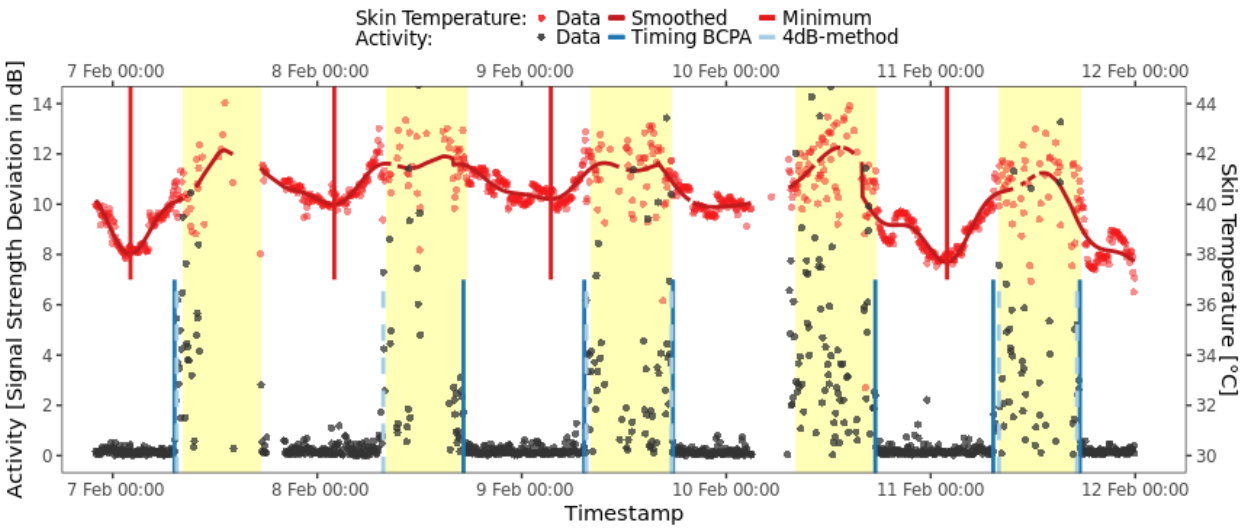

Figure S2_5: Skin temperature minima (red vertical lines) and chronotypes (i.e. onset and offset) for activity from BCPA (dark blue) and from 4dB-threshold method (light blue & dashed) added to the previous example showing patterns of activity (black dots) and skin temperature patterns (light red dots for filtered, and dark red line for smoothed data) across time. Yellow shades indicate daylight periods.

Full R codes for the processing pipeline are available upon request.

Session Info

```
## R version 4.3.1 (2023-06-16)
## Platform: x86_64-pc-linux-gnu (64-bit)
## Running under: Ubuntu 20.04.6 LTS
##
## Matrix products: default
## BLAS:   /usr/lib/x86_64-linux-gnu/openblas-pthread/libblas.so.3
## LAPACK: /usr/lib/x86_64-linux-gnu/openblas-pthread/liblapack.so.3;  LAPACK version 3.9.0
##
## locale:
##  [1] LC_CTYPE=en_US.UTF-8       LC_NUMERIC=C
##  [3] LC_TIME=en_US.UTF-8        LC_COLLATE=en_US.UTF-8
##  [5] LC_MONETARY=en_US.UTF-8    LC_MESSAGES=en_US.UTF-8
##  [7] LC_PAPER=en_US.UTF-8       LC_NAME=C
##  [9] LC_ADDRESS=C               LC_TELEPHONE=C
## [11] LC_MEASUREMENT=en_US.UTF-8 LC_IDENTIFICATION=C
##
## time zone: Europe/Amsterdam
## tzcode source: system (glibc)
##
## attached base packages:
## [1] stats     graphics  grDevices utils     datasets  methods   base
##
## other attached packages:
##  [1] scales_1.2.1   gridExtra_2.3  ggplot2_3.4.3  readr_2.1.4    suncalc_0.5.1
##  [6] chron_2.3-61   mclust_6.0.0   diptest_0.76-0 pracma_2.4.2   reshape2_1.4.4
## [11] tidyr_1.3.0    dplyr_1.1.2
##
## loaded via a namespace (and not attached):
##  [1] utf8_1.2.3       generics_0.1.3    stringi_1.7.12    hms_1.1.3
##  [5] digest_0.6.33    magrittr_2.0.3    evaluate_0.21     grid_4.3.1
##  [9] timechange_0.2.0 fastmap_1.1.1     plyr_1.8.8        purrr_1.0.2
## [13] fansi_1.0.4      cli_3.6.1         crayon_1.5.2      rlang_1.1.1
## [17] bit64_4.0.5      munsell_0.5.0     withr_2.5.0       yaml_2.3.7
## [21] parallel_4.3.1   tools_4.3.1       tzdb_0.4.0        colorspace_2.1-0
## [25] vctrs_0.6.3      R6_2.5.1          lifecycle_1.0.3   lubridate_1.9.2
## [29] stringr_1.5.0    bit_4.0.5         vroom_1.6.3       pkgconfig_2.0.3
## [33] pillar_1.9.0     gtable_0.3.4      data.table_1.14.8 glue_1.6.2
## [37] Rcpp_1.0.10      xfun_0.40         tibble_3.2.1      tidyselect_1.2.0
## [41] rstudioapi_0.15.0 knitr_1.43       farver_2.1.1      htmltools_0.5.6
## [45] labeling_0.4.2   rmarkdown_2.24    compiler_4.3.1
```

References

Jonasson, K. A. (2017) The effects of sex, energy, and environmental conditions on the movement ecology of migratory bats (Dissertation). *Electronic Thesis and Dissertation Repository*, 4411. http://ir.lib.uwo.ca/etd/4411

Strauß, A. F. T., McCafferty, D. J., Nord, A., Lehmann, M., & Helm, B. (2022) Using skin temperature and activity profiles to assign chronotype in birds. *Animal Biotelemetry*, 10(1). https://doi.org/10.1186/s40317-022-00296-w

Dominoni, D. M., Carmona-Wagner, E. O., Hofmann, M., Kranstauber, B., & Partecke, J. (2014) Individual-based measurements of light intensity provide new insights into the effects of artificial light at night on daily rhythms of urban-dwelling songbirds. *The Journal of Animal Ecology*, 83(3), 681–692. https://doi.org/10.1111/1365-2656.12150

Adelman, J. S., Córdoba-Córdoba, S., Spoelstra, K., Wikelski, M., & Hau, M. (2010) Radiotelemetry reveals variation in fever and sickness behaviours with latitude in a free-living passerine. *Functional Ecology*, 24, 813–823. https://doi.org/10.1111/j.1365-2435.2010.01702.x